

# SINGLE MESON PHOTOPRODUCTION AND IR RENORMALONS

Shahin S. Agaev\*

*International Centre for Theoretical Physics, Trieste, Italy*

## Abstract

Single pseudoscalar and vector mesons inclusive photoproduction  $\gamma h \rightarrow MX$  via higher twist mechanism is calculated using the QCD running coupling constant method. It is proved that in the context of this method a higher twist contribution to the photoproduction cross section cannot be normalized in terms of the meson electromagnetic form factor. The structure of infrared renormalon singularities of the higher twist subprocess cross section and the resummed expression (the Borel sum) for it are found. Comparisons are made with earlier results, as well as with leading twist cross section. Phenomenological effects of studied contributions for  $\pi$ ,  $K$ ,  $\rho$ -meson photoproduction are discussed.

---

\*Permanent address: High Energy Physics Lab., Baku State University, Z.Khalilov st. 23, 370148 Baku, Azerbaijan. E-mail: azhep@lan.ab.az

# 1 INTRODUCTION

One of the fundamental achievements of QCD is the prediction of asymptotic scaling laws for large-angle exclusive processes and their calculation in the framework of perturbative QCD (pQCD) [1-3]. In the context of the factorized QCD an expression for an amplitude of an exclusive process can be written as integral over  $\mathbf{x}, \mathbf{y}$  of hadron wave functions (w.f.)<sup>1</sup>  $\Phi_i(\mathbf{x}, \hat{Q}^2)$  (an initial hadron),  $\Phi_f^*(\mathbf{x}, \hat{Q}^2)$  (a final hadron) and amplitude  $T_H(\mathbf{x}, \mathbf{y}; \alpha_S(\hat{Q}^2), Q^2)$  of the hard-scattering subprocess [2]. The hard-scattering amplitude  $T_H(\mathbf{x}, \mathbf{y}; \alpha_S(\hat{Q}^2), Q^2)$  depends on a process and can be obtained in the framework of pQCD, whereas the w.f.  $\Phi(\mathbf{x}, \hat{Q}^2)$  describes all the non-perturbative and process-independent effects of hadronic binding. The hadron w.f. gives the amplitude for finding partons (quarks, gluons) carrying the longitudinal fractional momenta  $\mathbf{x} = (x_1, x_2, \dots, x_n)$  and virtualness up to  $\hat{Q}^2$  within the hadron and, in general, includes all Fock states with quantum numbers of the hadron. But only the lowest Fock state ( $q_1\bar{q}_2$  - for mesons,  $uud$  - for proton, etc.) contributes to the leading scaling behavior, other Fock states' contributions are suppressed by powers of  $1/Q^2$ . In our work we shall restrict ourselves by considering the lowest Fock state for a meson. Then,  $\mathbf{x} = x_1, x_2$  and  $x_1 + x_2 = 1$ .

This approach can be applied for investigation, not only exclusive processes but also for the calculation of higher twist (HT) corrections to some inclusive processes, such as large- $p_T$  dilepton production [4], two-jet+meson production in the electron-positron annihilation [5], etc. The HT corrections to a single meson inclusive photoproduction and jet photoproduction cross sections were studied by various authors [6,7]. In these early papers for calculation of integrals over  $\mathbf{x} = x_1, x_2$ , like

$$I \sim \int \alpha_S(\hat{Q}^2) \Phi(\mathbf{x}, \hat{Q}^2) F(\mathbf{x}, \alpha_S(\hat{Q}^2), Q^2) \delta(1 - x_1 - x_2) dx_1 dx_2 \quad (1)$$

which appear in an expression of the amplitude, the frozen coupling constant approximation was used. Some comments are in order concerning this point. It is well known [8], that in pQCD calculations the argument of the running coupling constant (or the renormalization and factorization scale)  $\hat{Q}^2$  should be taken equal to the square of the momentum transfer of a hard gluon in a corresponding Feynman diagram. But defined in this way,  $\alpha_S(\hat{Q}^2)$  suffers from infrared singularities. Indeed, in a meson form factor calculations, for example,  $\hat{Q}^2$  equals to  $x_1 y_1 Q^2$  or  $x_2 y_2 Q^2$ ,  $-Q^2$  being the four momentum square of the virtual photon. In the single meson photoproduction  $\gamma h \rightarrow MX$ , this scale has to be chosen equal to  $-x_1 \hat{u}$  or  $x_2 \hat{s}$ , where  $\hat{u}, \hat{s}$  are the subprocess's Mandelstam invariants [6]. Therefore, in the soft regions  $x_1 \rightarrow 0, y_1 \rightarrow 0; x_2 \rightarrow 0, y_2 \rightarrow 0$  or  $x_1 \rightarrow 0, x_2 \rightarrow 0$  integrals (1) diverge

---

<sup>1</sup>Strictly speaking,  $\Phi_M(\mathbf{x}, \hat{Q}^2)$  is a hadron distribution amplitude and it differs from a hadron wave function; the former can be obtained by integrating the corresponding wave function over partons' transverse momenta up to the factorization scale  $\hat{Q}^2$ . But in this paper we use these two terms on the same footing.

and for their calculation some regularization methods of  $\alpha_S(\hat{Q}^2)$  in these regions are needed. In the frozen coupling approximation these difficulties were avoided simply by equating  $\hat{Q}^2$  to some fixed quantity characterizing the process. In form factor calculations this is  $\hat{Q}^2 \equiv Q^2/4$  [9], in the single meson photoproduction -  $\hat{Q}^2 \equiv \hat{s}/2, -\hat{u}/2$  [6].

Recently, in our papers [10,11] devoted to the investigation of the light mesons electromagnetic form factors, for their calculation we applied the running coupling constant method, where these singularities had been regularized by means of the principal value prescription [12]. In our recent work we consider the inclusive photoproduction of single pseudoscalar and vector mesons  $\gamma h \rightarrow MX$  using the same approach.

## 2 CALCULATION OF THE HIGHER TWIST DIAGRAMS

The two HT subprocesses, namely  $\gamma q_1 \rightarrow M q_2$  and  $\gamma \bar{q}_2 \rightarrow M \bar{q}_1$  contribute to the photoproduction of the single meson  $M$  in the reaction  $\gamma h \rightarrow MX$ . The Feynman diagrams for the first subprocess are shown in *Fig.1*. We do not provide the set of diagrams corresponding to the second subprocess  $\gamma \bar{q}_2 \rightarrow M \bar{q}_1$ ; they can be obtained from *Fig.1* by exchanging the quark and antiquark lines. The momenta and charges of the particles in question are indicated in *Fig.1(a)*. In our investigation the meson mass is neglected. As is seen from *Fig.1*, in the HT subprocess the meson  $M$  is coupled directly to the photon and the hadron quark and its suppression in comparison with leading twist subprocesses is caused by a hard gluon exchange in the higher twist diagrams.

The amplitude for the subprocess  $\gamma q_1 \rightarrow M q_2$  can be found by means of the Brodsky-Lepage method [2],

$$M = \int_0^1 \int_0^1 dx_1 dx_2 \delta(1 - x_1 - x_2) T_H(x_1, x_2; \alpha_S(\hat{Q}^2), \hat{s}, \hat{u}, \hat{t}) \Phi_M(x_1, x_2; \hat{Q}^2) \quad (2)$$

In (2),  $T_H$  is the sum of graphs contributing to the hard-scattering part of the subprocess, which for the subprocess under consideration is  $\gamma + q_1 \rightarrow (q_1 \bar{q}_2) + q_2$ , where a quark and antiquark from the meson form a color singlet state  $(q_1 \bar{q}_2)$ .

The important ingredient of our study is the choice of the meson model w.f.  $\Phi_M$ . In this work we calculate the photoproduction of the pseudoscalar (pion, kaon) and vector ( $\rho$ -meson) mesons. For these mesons in the literature [3],[13] various w.f. were proposed. Here for the pion and kaon we use the phenomenological w.f. obtained in [3] by applying the QCD sum rules method, for calculation of the  $\rho$ -meson photoproduction we utilize both w.f. found in [3] and derived in [13]. The reason is that, in accordance with results of Ref.[13], the wave functions of longitudinally and transversely polarized  $\rho$ -mesons are similar (coincide in shape),

whereas in [3] a significant difference between them was predicted. In [13] the authors suggested also that the change in shape of the transverse  $\rho$ -meson w.f. may increase the rate of the production of transversely polarized  $\rho$ -mesons by a factor 2. We think that the single meson photoproduction is a suitable arena for checking this conclusion.

The pion and  $\rho$ -meson wave functions have the form

$$\Phi_M(x, \mu_0^2) = \Phi_{asy}^M(x) [a + b(2x - 1)^2]. \quad (3)$$

For the model w.f. the coefficients  $a, b$  take the following values: Chernyak-Zhitnitsky w.f. [3];

$$\begin{aligned} a &= 0, b = 5, \quad \text{for the pion,} \\ a &= 0.7, b = 1.5, \quad \text{for the longitudinally polarized } \rho_L \text{ - meson,} \\ a &= 1.25, b = -1.25, \quad \text{for the transversely polarized } \rho_T \text{ - meson.} \end{aligned} \quad (4)$$

Ball-Braun w.f.[13];

$$a = 0.7, \quad b = 1.5,$$

for both longitudinally and transversely polarized  $\rho$ -meson. Here we have denoted by  $x \equiv x_1$  the longitudinal fractional momentum carrying by the quark within the meson. Then,  $x_2 = 1 - x$  and  $x_1 - x_2 = 2x - 1$ .

The pion and  $\rho$ -meson w.f. are symmetric under replacement  $x_1 - x_2 \leftrightarrow x_2 - x_1$ . But the kaon w.f. is non-symmetric;  $\Phi_K(x_1 - x_2) \neq \Phi_K(x_2 - x_1)$  [3]. Indeed, the kaon w.f. includes a term proportional to odd power of  $(2x - 1)$ ,

$$\begin{aligned} \Phi_K(x, \mu_0^2) &= \Phi_{asy}^K(x) [a + b(2x - 1)^2 + c(2x - 1)^3], \\ a &= 0.4, \quad b = 3, \quad c = 1.25, \end{aligned} \quad (5)$$

and may be written as the sum of the symmetric  $\Phi_s(x, \mu_0^2)$  and antisymmetric  $\Phi_a(x, \mu_0^2)$  parts,

$$\Phi_s(x, \mu_0^2) = \Phi_{asy}^K(x) [a + b(2x - 1)^2], \quad \Phi_a(x, \mu_0^2) = \Phi_{asy}^K(x)c(2x - 1)^3. \quad (6)$$

In (3),(5),(6)  $\Phi_{asy}^M(x)$  is the asymptotic w.f.

$$\Phi_{asy}^M(x) = \sqrt{3}f_M x(1 - x), \quad (7)$$

where  $f_M$  is the meson decay constant;  $f_\pi = 0.093 \text{ GeV}$ ,  $f_K = 0.112 \text{ GeV}$ . In the case of the  $\rho$ -meson we take  $f_\rho^L = f_\rho^T = 0.2 \text{ GeV}$  for the CZ w.f., and  $f_\rho^L = 0.2 \text{ GeV}$ ,  $f_\rho^T = 0.16 \text{ GeV}$  for BB w.f.

The normalization of  $\Phi_M(x, \mu_0^2)$  at  $\mu_0 = 0.5 \text{ GeV}$  is given by the condition

$$\int_0^1 dx \Phi_M(x, \mu_0^2) = \frac{f_M}{2\sqrt{3}}. \quad (8)$$

The factor  $\sqrt{2}$  appearing in the normalization of a vector meson is included in the  $\rho$ -meson decay constant.

The formalism for calculation of the HT subprocess cross section is well known and described in [6,14]. We omit details of our calculations and write down the final expression for  $d\hat{\sigma}^{HT}/d\hat{t}$ . We find:

for the pseudoscalar and longitudinally polarized vector mesons,

$$\begin{aligned} \frac{d\hat{\sigma}^{HT}(e_1, e_2)}{d\hat{t}} &= \frac{32\pi^2 C_F \alpha_E}{9\hat{s}^2} \left\{ -\frac{e_1^2}{\hat{s}^2} \left[ I_1^2 \hat{t} - 2I_1 (I_1 \hat{s} + I_2 \hat{u}) \frac{\hat{u}}{\hat{t}} + I_2^2 \frac{\hat{u}^2}{\hat{t}} \right] - \right. \\ &\quad \frac{e_2^2}{\hat{u}^2} \left[ K_1^2 \hat{t} - 2K_1 (K_1 \hat{u} + K_2 \hat{s}) \frac{\hat{s}}{\hat{t}} + K_2^2 \frac{\hat{s}^2}{\hat{t}} \right] - \\ &\quad \left. \frac{2e_1 e_2}{\hat{s}\hat{u}\hat{t}} \left[ I_1 K_1 \hat{t}^2 - I_1 (K_2 \hat{s} + K_1 \hat{u}) \hat{s} - K_1 (I_1 \hat{s} + I_2 \hat{u}) \hat{u} \right] \right\}. \end{aligned} \quad (9)$$

for the transversely polarized vector meson,

$$\frac{d\hat{\sigma}^{HT}(e_1, e_2)}{d\hat{t}} = \frac{64\pi^2 C_F \alpha_E}{9\hat{s}^4} \frac{-\hat{t}}{\hat{u}^2} [e_1 \hat{u} I_2 - e_2 \hat{s} K_2]^2 \quad (10)$$

In (9),(10),  $\alpha_E \simeq 1/137$  is the fine structure constant,  $C_F = 4/3$  is the color factor. The Mandelstam invariants for the subprocess are defined as

$$\begin{aligned} \hat{s} &= (zp + q)^2 = zs, \\ \hat{t} &= (q - P)^2 = t, \\ \hat{u} &= (zp - P)^2 = zu, \end{aligned} \quad (11)$$

where  $s, t, u$  are the Mandelstam invariants for the process  $\gamma h \rightarrow MX$ ,  $z$  is the longitudinal fractional momentum of the quark  $q_1$  out of the hadron  $h$ .

The main problem in our investigation is the calculation of quantities  $I_{1,2}, K_{1,2}$ ,

$$I_1 = \int_0^1 \int_0^1 \frac{dx_1 dx_2 \delta(1 - x_1 - x_2) \alpha_S(\hat{Q}_1^2) \Phi_M(x_1, x_2; \hat{Q}_1^2)}{x_2}, \quad (12)$$

$$I_2 = \int_0^1 \int_0^1 \frac{dx_1 dx_2 \delta(1 - x_1 - x_2) \alpha_S(\hat{Q}_1^2) \Phi_M(x_1, x_2; \hat{Q}_1^2)}{x_1 x_2}, \quad (13)$$

and

$$K_1 = \int_0^1 \int_0^1 \frac{dx_1 dx_2 \delta(1 - x_1 - x_2) \alpha_S(\hat{Q}_2^2) \Phi_M(x_1, x_2; \hat{Q}_2^2)}{x_1}, \quad (14)$$

$$K_2 = \int_0^1 \int_0^1 \frac{dx_1 dx_2 \delta(1 - x_1 - x_2) \alpha_S(\hat{Q}_2^2) \Phi_M(x_1, x_2; \hat{Q}_2^2)}{x_2}, \quad (15)$$

where for  $I_1, I_2$  the renormalization and factorization scale is  $\widehat{Q}_1^2 = x_2 \widehat{s}$ , for  $K_1, K_2$  it is given by  $\widehat{Q}_2^2 = -x_1 \widehat{u}$ .

Let us first consider the frozen coupling constant approximation. In this approximation we put  $\widehat{Q}_{1,2}^2$  equal to their mean values  $\widehat{s}/2, -\widehat{u}/2$  and remove  $\alpha_S(\widehat{Q}_{1,2}^2)$  as the constant factor in (12-15). After such manipulation, the integrals (12-15) are trivial and can easily be found. For the mesons with symmetric w.f. we get

$$\begin{aligned} I_2^0\left(\frac{\widehat{s}}{2}\right) &= 2I_1^0\left(\frac{\widehat{s}}{2}\right) \equiv \alpha_S\left(\frac{\widehat{s}}{2}\right) I_M\left(\frac{\widehat{s}}{2}\right), \\ K_2^0\left(-\frac{\widehat{u}}{2}\right) &= 2K_1^0\left(-\frac{\widehat{u}}{2}\right) \equiv \alpha_S\left(-\frac{\widehat{u}}{2}\right) I_M\left(-\frac{\widehat{u}}{2}\right), \end{aligned}$$

where superscript "0" indicates that the quantities  $I, K$  are found in the frozen coupling approximation. Here the function  $I_M(\widehat{Q}^2)$  is

$$I_M(\widehat{Q}^2) = \int_0^1 \frac{dx \Phi_M(x, \widehat{Q}^2)}{x(1-x)}.$$

In this approximation, using the last expressions and (9),(10),(12-15) one can easily reproduce results of [6] for the subprocess cross section<sup>2</sup>.

In the case of the kaon we find

$$\begin{aligned} I_1^0\left(\frac{\widehat{s}}{2}\right) &= \alpha_S\left(\frac{\widehat{s}}{2}\right) \left[ \int_0^1 \frac{dx \Phi_s(x, \widehat{s}/2)}{1-x} + \int_0^1 \frac{dx \Phi_a(x, \widehat{s}/2)}{1-x} \right], \\ I_2^0\left(\frac{\widehat{s}}{2}\right) &= 2\alpha_S\left(\frac{\widehat{s}}{2}\right) \int_0^1 \frac{dx \Phi_s(x, \widehat{s}/2)}{1-x}. \end{aligned} \quad (16)$$

It is evident that

$$I_2^0(\widehat{s}/2) \neq 2I_1^0(\widehat{s}/2).$$

The same is also true for  $K_1^0$  and  $K_2^0$ . This means that in the case of a pseudoscalar meson with the non-symmetric w.f. the result of [6] is not valid and in the calculations our expressions (9),(12-15) have to be applied.

The important problem in the single meson inclusive photoproduction is the possibility of normalization of the HT subprocess cross section (9),(10) in terms of the electromagnetic form factor  $F_M(Q^2)$  of the corresponding meson.

The electromagnetic form factor  $F_M(Q^2)$  of the meson  $M$  is given by the expression

$$F_M(Q^2) = \int_0^1 \int_0^1 \Phi_M^*(y, \widehat{Q}^2) T_H^{ff}(x, y; \alpha_S(\widehat{Q}^2), Q^2) \Phi_M(x, \widehat{Q}^2) dx dy. \quad (17)$$

---

<sup>2</sup>The difference between our expressions and corresponding formulas in Ref.[6] is caused by our definition of the antiquark's charge, i.e. in our expressions the charge of the antiquark from  $M$  is  $-e_2$ , whereas in Ref.[6] it is denoted by  $e_2$ .

Here

$$T_H^{ff}(x, y; \alpha_S(\widehat{Q}^2), Q^2) = \frac{16\pi C_F}{Q^2} \left[ e_1 \frac{\alpha_S(Q^2(1-x)(1-y))}{(1-x)(1-y)} - e_2 \frac{\alpha_S(Q^2 xy)}{xy} \right].$$

For the meson with symmetric w.f. using the frozen coupling approximation ( $\widehat{Q}^2 \rightarrow Q^2/4$ ) we get

$$F_M(Q^2) = \frac{16\pi C_F \alpha_S(Q^2/4)}{Q^2} (e_1 - e_2) \left( \int_0^1 \frac{\Phi_M(x, Q^2/4) dx}{1-x} \right)^2. \quad (18)$$

It is not difficult to conclude that for such mesons the quantities  $(I^0)^2$  and  $(K^0)^2$  in the cross section can be expressed in terms of  $F_M$

$$[I_1^0(\widehat{s}/2)]^2 = \frac{\alpha_S(\widehat{s}/2)}{16\pi C_F} \left[ Q^2 |F_M(Q^2)| \right] \Big|_{\widehat{Q}^2=2\widehat{s}} \quad (19)$$

$$[I_2^0(\widehat{s}/2)]^2 = \frac{\alpha_S(\widehat{s}/2)}{4\pi C_F} \left[ Q^2 |F_M(Q^2)| \right] \Big|_{\widehat{Q}^2=2\widehat{s}}$$

For mesons with non-symmetric w.f. from (17) we find

$$\begin{aligned} F_M(Q^2) = & \frac{16\pi C_F \alpha_S(Q^2/4)}{Q^2} \left\{ (e_1 - e_2) \left( \int_0^1 \frac{\Phi_s(x, Q^2/4) dx}{1-x} \right)^2 + \right. \\ & (e_1 - e_2) \left( \int_0^1 \frac{\Phi_a(x, Q^2/4) dx}{1-x} \right)^2 + \\ & \left. 2(e_1 + e_2) \left( \int_0^1 \frac{\Phi_s(x, Q^2/4) dx}{1-x} \right) \left( \int_0^1 \frac{\Phi_a(x, Q^2/4) dx}{1-x} \right) \right\}. \quad (20) \end{aligned}$$

It is now clear that  $(I^0)^2, (K^0)^2$  (16) are not proportional to  $F_M$  (20). This means that even in the context of the frozen coupling approximation the HT subprocess cross section may be normalized in terms of the meson form factor only if the photoproduction of the meson with symmetric w.f. is considered.

### 3 THE RUNNING COUPLING CONSTANT METHOD AND IR RENORMALONS

In this section we shall calculate the integrals (12-15) using the running coupling constant method and also discuss the problem of normalization of the higher twist process cross section in terms of the meson electromagnetic form factor obtained in the context of the same approach.

As is seen from (12-15), in general, one has to take into account not only the dependence of  $\alpha(\hat{Q}_{1,2}^2)$  on the scale  $\hat{Q}_{1,2}^2$ , but also an evolution of  $\Phi_M(x, \hat{Q}_{1,2}^2)$  with  $\hat{Q}_{1,2}^2$ . The meson w.f. evolves in accordance with a Bethe-Salpeter type equation, but its dependence on  $\hat{Q}^2$  is mild and may be neglected by replacing  $\Phi_M(x, \hat{Q}_{1,2}^2) \rightarrow \Phi_M(x, \mu_0^2)$ . Such approximation does not change considerably numerical results, but phenomenon considering in this article (effect of infrared renormalons) becomes transparent.

Let us clarify our method by calculating the integral (12); the quantities  $I_2, K_{1,2}$  can be worked out in the same way. For the mesons with symmetric w.f. Eq.(12) in the framework of the running coupling approach takes the form

$$I_1(\hat{s}) = \int_0^1 \frac{\alpha_S((1-x)\hat{s})\Phi_M(x, \mu_0^2)dx}{1-x}. \quad (21)$$

The  $\alpha_S((1-x)\hat{s})$  has the infrared singularity at  $x \rightarrow 1$  and as a result integral (21) diverges (the pole associated with the denominator of the integrand is fictitious, because  $\Phi_M \sim (1-x)$ , and therefore, the singularity of the integrand at  $x = 1$  is caused only by  $\alpha_S((1-x)\hat{s})$ ). For the regularization of the integral let us relate the running coupling at scaling variable  $\alpha_S((1-x)\hat{s})$  with the aid of the renormalization group equation in terms of the fixed one  $\alpha_S(\hat{s})$ . The renormalization group equation for the running coupling  $\alpha(\hat{s}) \equiv \alpha_S(\hat{s})/\pi$

$$\frac{\partial \alpha(\lambda\hat{s})}{\partial \ln \lambda} \simeq -\frac{\beta_0}{4} [\alpha(\lambda\hat{s})]^2, \quad (22)$$

has the solution [12]

$$\alpha(\lambda\hat{s}) \simeq \frac{\alpha(\hat{s})}{1 + (\alpha(\hat{s})\beta_0/4) \ln \lambda}. \quad (23)$$

In (22),(23), the one-loop QCD coupling constant  $\alpha_S(\mu^2)$  is defined as

$$\alpha_S(\mu^2) = \frac{4\pi}{\beta_0 \ln(\mu^2/\Lambda^2)}$$

$\beta_0 = 11 - 2n_f/3$  being the QCD beta-function first coefficient.

Having inserted (23) into (21) we get

$$I_1(\hat{s}) = \alpha_S(\hat{s}) \int_0^1 \frac{\Phi_M(x, \mu_0^2) dx}{(1-x)(1+(1/t)\ln(1-x))}, \quad (24)$$

where  $t = 4\pi/\alpha_S(\hat{s})\beta_0$ .

The integral (24) is, of course, still divergent, but now it is recasted into a form, which is suitable for calculation. Using the method described in details in our work [10] it may be found as a perturbative series in  $\alpha_S(\hat{s})$

$$I_1(\hat{s}) \sim \sum_{n=1}^{\infty} \left( \frac{\alpha_S(\hat{s})}{4\pi} \right)^n S_n, \quad S_n = C_n \beta_0^{n-1}. \quad (25)$$

The coefficients  $C_n$  of this series demonstrate factorial growth  $C_n \sim (n-1)!$ , which might indicate an infrared renormalon nature of divergences in the integral (24) and corresponding series (25). The procedure for dealing with such ill-defined series is well known; one has to perform the Borel transform of the series [15]

$$B[I_1](u) = \sum_{n=1}^{\infty} \frac{u^{n-1}}{(n-1)!} C_n, \quad (26)$$

then invert  $B[I_1](u)$  to obtain the resummed expression (the Borel sum) for  $I_1(\hat{s})$ . This method is straightforward but tedious. Therefore, it is convenient to apply the second method proposed also in our work [11], which allows us to bypass all these intermediate steps and find directly the resummed expression for  $I_1(\hat{s})$ . For these purposes let us introduce the inverse Laplace transform of  $1/(t+z)$

$$\frac{1}{t+z} = \int_0^{\infty} \exp[-(t+z)u] du. \quad (27)$$

Then  $I_1(\hat{s})$  may be readily carried out by the change of the variable  $x$  to  $z = \ln(1-x)$  and using (27)

$$I_1(\hat{s}) = \frac{4\sqrt{3}\pi f_M}{\beta_0} \int_0^{\infty} \exp\left[-\frac{4\pi u}{\alpha_S(\hat{s})\beta_0}\right] \left( \frac{a+b}{1-u} - \frac{a+5b}{2-u} + \frac{8b}{3-u} - \frac{4b}{4-u} \right). \quad (28)$$

Eq.(28) is nothing more than the Borel sum of the perturbative series (25) and the corresponding Borel transform is

$$B[I_1](u) = \frac{a+b}{1-u} - \frac{a+5b}{2-u} + \frac{8b}{3-u} - \frac{4b}{4-u}. \quad (29)$$

The series (25) can be recovered by means of the following formula

$$C_n = \left( \frac{d}{du} \right)^{n-1} B[I_1](u) \Big|_{u=0} .$$

The Borel transform  $B[I_1](u)$  has poles on the real  $u$  axis at  $u = 1; 2; 3; 4$ , which confirms our conclusion concerning the infrared renormalon nature of divergences in (25). To remove them from Eq.(28) some regularization methods have to be applied. In this article we adopt the principal value prescription [12]. We obtain

$$\begin{aligned} [I_1(\hat{s})]^{res} = & \frac{4\sqrt{3}\pi f_M}{\beta_0} \left[ (a+b) \frac{Li(\lambda)}{\lambda} - (a+5b) \frac{Li(\lambda^2)}{\lambda^2} + \right. \\ & \left. 8b \frac{Li(\lambda^3)}{\lambda^3} - 4b \frac{Li(\lambda^4)}{\lambda^4} \right], \end{aligned} \quad (30)$$

where  $Li(\lambda)$  is the logarithmic integral [16], for  $\lambda > 1$  defined in its principal value

$$Li(\lambda) = P.V. \int_0^\infty \frac{dx}{\ln x}, \quad \lambda = \hat{s}/\Lambda^2. \quad (31)$$

For other integrals from (13-15) we find

$$[I_2(\hat{s})]^{res} = \frac{4\sqrt{3}\pi f_M}{\beta_0} \left[ (a+b) \frac{Li(\lambda)}{\lambda} - 4b \frac{Li(\lambda^2)}{\lambda^2} + 4b \frac{Li(\lambda^3)}{\lambda^3} \right], \quad (32)$$

and

$$[K_1(-\hat{u})]^{res} = [I_1(-\hat{u})]^{res}, \quad [K_2(-\hat{u})]^{res} = [I_2(-\hat{u})]^{res}. \quad (33)$$

From (30),(32),(33), we conclude that in the framework of the running coupling approximation even for mesons with symmetric w.f. we have

$$[I_2(\hat{s})]^{res} \not\sim [I_1(\hat{s})]^{res}, \quad [K_2(-\hat{u})]^{res} \not\sim [K_1(-\hat{u})]^{res}.$$

Therefore only our results for the subprocess cross section (9),(10) are correct.

Another question is, as we have discussed in Sect.2, the normalization of the meson photoproduction cross section in terms of the meson elm form factor. The pion and kaon form factors have been calculated by means of the running coupling approach in our previous papers [10, 11]. Let us write down the pion form factor obtained using the pion's simplest w.f., that is, the asymptotic one ( $a = 1, b = 0$  in (4))

$$[Q^2 F_\pi(Q^2)]_{asy}^{res} = \frac{(16\pi f_\pi)^2}{\beta_0} \left[ -\frac{3}{2} + (\ln \lambda - 2) \frac{Li(\lambda)}{\lambda} + (\ln \lambda + 2) \frac{Li(\lambda^2)}{\lambda^2} \right]. \quad (34)$$

From (30),(34) it follows that the relations (19) do no longer hold. The same is also true for the pion's other w.f., as well as for  $\rho_L$ - and  $\rho_T$ -mesons. In other words, in the running coupling approach the HT subprocess cross section (9),(10) cannot be normalized in terms of the meson form factor neither for mesons with symmetric w.f. nor for non-symmetric ones.

Let us, for completeness, write down  $I(\hat{s}), K(-\hat{u})$  calculated for non-symmetric w.f. (5)

$$[I_1(\hat{s})]^{res} = \frac{4\sqrt{3}\pi f_M}{\beta_0} \left[ (a+b+c) \frac{Li(\lambda)}{\lambda} - (a+5b+7c) \frac{Li(\lambda^2)}{\lambda^2} + 2(4b+9c) \frac{Li(\lambda^3)}{\lambda^3} - 4(b+5c) \frac{Li(\lambda^4)}{\lambda^4} + 8c \frac{Li(\lambda^5)}{\lambda^5} \right], \quad (35)$$

$$[I_1(\hat{s})]^{res} = \frac{4\sqrt{3}\pi f_M}{\beta_0} \left[ (a+b+c) \frac{Li(\lambda)}{\lambda} - 2(2b+3c) \frac{Li(\lambda^2)}{\lambda^2} + 4(b+3c) \frac{Li(\lambda^3)}{\lambda^3} - 8c \frac{Li(\lambda^4)}{\lambda^4} \right]. \quad (36)$$

The expressions for  $[K_1(-\hat{u})]^{res}$  and  $[K_2(-\hat{u})]^{res}$  may be obtained from (35),(36) by  $c \rightarrow -c, \lambda = \hat{s}/\Lambda^2 \rightarrow -\hat{u}/\Lambda^2$  replacements, respectively. With these explicit expressions and the results of [11] at hand one can check our statements concerning the normalization of the subprocess cross section for kaons.

Some comments are in order concerning these results. First of all, it is instructive to compare sources of the infrared renormalons in our case and in other QCD processes considered in [17]. In these articles the running coupling constant method was used in one-loop order calculations for resummation of any number of fermion bubble insertions in the gluon propagator. This technique corresponds to partial resummation of the perturbative series for a quantity under consideration. Indeed, for such quantities, the coefficients  $S_n$  in (25) have the following expansion in powers of  $\beta_0$ ,

$$S_n = C_n \beta_0^{n-1} + R_n \beta_0^{n-2} + \dots$$

Therefore, by defining the Borel transform as in (26) and inverting it one obtains a partially resummed expression for a physical quantity. In our calculations of the HT cross section we use the leading order term for  $T_H$ ; there are no gluon loops in the corresponding Feynman diagrams in *Fig.1*. It is not accidental that  $S_n$  (25) in our case has exactly  $\sim \beta_0^{n-1}$  dependence and, hence, the expressions (30),(32),(35),(36) are exact sums of the corresponding perturbative series. In [17] it has been demonstrated that the only source of terms of order  $\sim \alpha_S^n \beta_0^{n-1}$  in (25) is the running coupling constant. The source of these terms in the HT calculations is also the running coupling  $\alpha_S(\hat{s}(1-x))$  (or  $\alpha_S(-\hat{u}(1-x))$ ), which runs due to

the integration in (1) over the meson quark's (antiquark's) longitudinal fractional momentum, but not because of a loop integration.

Another question commonly discussed in papers involving IR renormalons is an ambiguity produced by the principal value prescription used for the regularization of divergent integrals (28). The ambiguity introduced by our treatment of (28) is a higher twist and behaves as  $\Lambda^2/\hat{Q}^2$  (the first renormalon pole is  $u = 1$ ). But the subprocess under consideration itself is already the higher twist one. Therefore, we can safely ignore such "HT-to-HT" corrections.

At the end of this section let us write down the HT correction to the single meson photoproduction cross section by taking into account both HT subprocesses;  $\gamma q_1 \rightarrow M q_2$  and  $\gamma \bar{q}_2 \rightarrow M \bar{q}_1$ . It is not difficult to prove that the second subprocess cross section can be obtained from (9),(10) by  $e_1 \leftrightarrow e_2$  replacement. Then the HT correction to the single meson photoproduction cross section is given by

$$\frac{\sigma^{HT}}{dp_T^2 dy} = z^* \sum_{q_1, \bar{q}_2} \left\{ q_1^h(z^*, -t) \frac{d\hat{\sigma}^{HT}(e_1, e_2)}{d\hat{t}} + \bar{q}_2^h(z^*, -t) \frac{d\hat{\sigma}^{HT}(e_2, e_1)}{d\hat{t}} \right\} \frac{s}{s+u}. \quad (37)$$

where

$$z^* = \frac{p_T e^{-y}}{\sqrt{s} - p_T e^y}.$$

Here the sum runs over the hadron's quark  $q_1$  and antiquark  $\bar{q}_2$  flavors. In (37)  $q_1^h(z^*, -t)$ ,  $\bar{q}_2^h(z^*, -t)$  are the quark and antiquark distribution functions, respectively. All r.h.s. quantities are expressed in terms of the process c.m. energy  $\sqrt{s}$ , the meson transverse momentum  $p_T$  and rapidity  $y$  using the following expressions

$$\hat{s} = \frac{sp_T e^{-y}}{\sqrt{s} - p_T e^y}, \quad \hat{t} = -p_T \sqrt{s} e^{-y}, \quad \hat{u} = -\frac{p_T^2 \sqrt{s}}{\sqrt{s} - p_T e^y}. \quad (38)$$

Eq.(37) is the final result which will be used later in our numerical calculations.

## 4 PHOTOPRODUCTION OF MESONS AT THE LEADING TWIST LEVEL

In our study of the single meson photoproduction a crucial point is the comparison of our results with leading twist (LT) ones. This will enable us to find such domains in the phase space in which the higher twist photoproduction mechanism is actually observable.

The LT subprocesses, which contribute to a meson photoproduction are: a photon-quark (antiquark) scattering

$$\gamma(q) + q_i(p_1) \rightarrow q_i(p_2) + g(p_3), \quad (\gamma \bar{q}_i \rightarrow \bar{q}_i g), \quad (39)$$

and photon-gluon fusion reactions

$$\gamma(q) + g(p_1) \rightarrow q_i(p_2) + \bar{q}_i(p_3). \quad (40)$$

In this article we consider the inclusive cross section difference in the photon-proton collision, namely

$$\Delta_M = \frac{d\sigma}{dp_T^2 dy}(\gamma p \rightarrow M^+ X) - \frac{d\sigma}{dp_T^2 dy}(\gamma p \rightarrow M^- X) \equiv \Sigma_{M^+} - \Sigma_{M^-}. \quad (41)$$

The LT subprocess which dominates in this difference is  $\gamma q \rightarrow gq$  with  $q \rightarrow M$ . Its cross section at the tree level is well known,

$$\frac{d\hat{\sigma}^{LT}}{d\hat{t}} = -\frac{8\pi\alpha_E e_q^2}{3\hat{s}^2} \left[ \alpha_S(\hat{s}) \frac{\hat{t}}{\hat{s}} + \alpha_S(-\hat{t}) \frac{\hat{s}}{\hat{t}} \right], \quad (42)$$

where the Mandelstam invariants of the subprocess are

$$\hat{s} = (q + p_1)^2, \quad \hat{t} = (q - p_2)^2, \quad \hat{u} = (q - p_3)^2.$$

In (42), the running coupling constant  $\alpha_S$  is evaluated at momentum scales  $\hat{s}$  and  $|\hat{t}|$ , which are equal to off-shell momenta carried by the virtual quark propagators in the corresponding Feynman diagrams of the leading twist subprocess  $\gamma q \rightarrow gq$ .

Many other subprocesses contribute to the meson photoproduction, among them i)  $\gamma q \rightarrow gq$  with  $g \rightarrow M$ , ii)  $\gamma \bar{q} \rightarrow g\bar{q}$  with  $\bar{q} \rightarrow M$ , iii)  $\gamma \bar{q} \rightarrow g\bar{q}$  with  $g \rightarrow M$ , iv)  $\gamma g \rightarrow q\bar{q}$  with  $q \rightarrow M$  or  $\bar{q} \rightarrow M$ . Considering the cross section difference  $\Delta_M$  we not only reduce the number of subprocesses contributing to  $\Delta_M$ , because the subprocesses involving gluons or antiquarks contribute equally to  $\Sigma_{M^+}^{LT}$  and  $\Sigma_{M^-}^{LT}$  and cancel in  $\Delta_M^{LT}$ , but also solve two other important problems. The first one is the next-to-leading order correction to the meson photoproduction cross section calculated in [18]. In this paper the authors have investigated the ratio

$$C^{\pi^+ - \pi^-} = \frac{d\sigma^{HO}(\gamma p \rightarrow \pi^+ X)/d\mathbf{p}_T dy - d\sigma^{HO}(\gamma p \rightarrow \pi^- X)/d\mathbf{p}_T dy}{d\sigma^{Born}(\gamma p \rightarrow \pi^+ X)/d\mathbf{p}_T dy - d\sigma^{Born}(\gamma p \rightarrow \pi^- X)/d\mathbf{p}_T dy} = K - 1,$$

for the cross section difference as a function of  $p_T$  at  $\sqrt{s} = 14.1 \text{ GeV}$  and  $y = 0.5$ . They have found that this ratio is negative and almost constant with  $p_T$  ( $p_T = 2 - 6 \text{ GeV}/c$ ). This means that the K-factor for the cross section difference is less than 1. In other words, using the LT cross section (42) for calculations of  $R_M = |\Delta_M^{HT}/\Delta_M^{LT}|$  at the same or slightly different kinematic regimes, we only underestimate the ratio  $R_M$  and related quantities and give lower bounds for them. The second problem solved by our choice of  $\Delta_M$  is a contribution to the photoproduction cross section originating from the photon's quark and gluon content. It is well known that the photoproduction process  $\gamma p \rightarrow h + X$  may proceed via two distinct mechanisms; photon can interact either directly with the hadron's

partons (direct photoproduction), or via its quark and gluon content (resolved photoproduction). As was demonstrated in [18], the contribution from the resolved photoproduction almost completely cancel in the  $\pi^+ - \pi^-$  difference. These results obtained in [18] for pions at certain kinematic domain seemingly are valid also for other light mesons at the same or slightly different kinematic conditions.

Then the leading twist contribution to the single meson photoproduction in  $\gamma p \rightarrow MX$  is given by the expression,

$$\frac{d\sigma^{LT}}{dp_T^2 dy} = \sum_q \int_{x_{min}}^1 \frac{dx q_p(x, -\hat{t}) D_{M/q}(z, -\hat{t})}{z} \frac{d\hat{\sigma}^{LT}}{d\hat{t}}, \quad (43)$$

where

$$z = \frac{p_T e^{-y}}{x\sqrt{s}} + \frac{p_T e^y}{\sqrt{s}}, \quad x_{min} = \frac{p_T e^{-y}}{\sqrt{s} - p_T e^y}. \quad (44)$$

In (43),  $q_p(x, -\hat{t})$  and  $D_{M/q}(z, -\hat{t})$  are a quark  $q$  distribution and fragmentation functions, respectively. The subprocess invariants  $\hat{s}$ ,  $\hat{t}$ ,  $\hat{u}$  in (43) are functions of  $s$ ,  $p_T$ ,  $y$ ,

$$\hat{s} = xs, \quad \hat{t} = -\frac{p_T \sqrt{s} e^{-y}}{z}, \quad \hat{u} = -\frac{xp_T \sqrt{s} e^y}{z}. \quad (45)$$

Eq.(43) together with (37) for the HT contributions will be applied in the next section for numerical calculations.

## 5 NUMERICAL RESULTS

In this section we compute the  $\gamma p \rightarrow M^+ X$  and  $\gamma p \rightarrow M^- X$  inclusive cross sections  $\Sigma_{M^+}$ ,  $\Sigma_{M^-}$ , as well as the difference  $\Delta_M = \Sigma_{M^+} - \Sigma_{M^-}$  by taking into account the dominant LT ( $\gamma q \rightarrow gq$  with  $q \rightarrow M$ ), and HT ( $\gamma q \rightarrow Mq$ ) contributions to the inclusive photoproduction. Only the HT cross section of  $K^-$  photoproduction is calculated using the proton  $s$  and  $\bar{u}$  quarks induced subprocesses, which contribute at the same order. Our calculations are performed for  $M = \pi, K, \rho$  at  $\sqrt{s} = 14.1 \text{ GeV}, 25 \text{ GeV}$ .

In this work, for quark distribution functions, we borrow the leading order parametrization of Owens [19]. This parametrization is suitable for our purposes, because the HT mechanism probe the quark distribution functions at  $z^* = p_T \exp(-y)/\sqrt{s} - p_T \exp(y)$ , which for chosen process's parameters is always more than 0.01. The same is also true for  $x_{min}$  in the LT cross section (43). That is, kinematical conditions allow us to avoid the region of small  $x \leq 0.01$ , where Owen's parametrization may give incorrect results. The same reason will enable us to compute  $\Sigma_M^{LT}$  ignoring a contribution from the leading twist subprocess  $\gamma g \rightarrow q\bar{q}$ , which otherwise may be considerable.

The quark fragmentation functions are taken from [20]. Recently, in [21], a new set of fragmentation functions for charged pions and kaons, both at leading and next-to-leading order, have been presented. These functions give  $D_q^{M^+M^-}(x, Q^2)$ , but not  $D_q^{M^\pm}(x, Q^2)$ . Therefore, we cannot apply them in our calculations.

The other problem is a choice of the QCD scale parameter  $\Lambda$  and number of active quark flavors  $n_f$ . The HT subprocesses probe the meson w.f. over a large range of  $Q^2$ ,  $Q^2$  being equal to  $\hat{s}$  or  $-\hat{u}$ . It is easy to find that  $-\hat{u}_{min} > 4.04 \text{ GeV}^2$ , while  $\hat{s}_{min} > 16 \text{ GeV}^2$ . For momentum scales  $\hat{s}$ ,  $-\hat{t}$  used in (42) as arguments of  $\alpha_S$  in the LT cross section we get

$$-\hat{t}_{min} > 6 \text{ GeV}^2, \quad \hat{s}_{min} > 16 \text{ GeV}^2.$$

In other kinematic domains these scales take essentially larger values. Taking into account these facts we find it reasonable to assign  $\Lambda = 0.1 \text{ GeV}$ ,  $n_f = 5$  throughout in this section.

Results of our numerical calculations are plotted in *Figs.2 – 8*. First of all, it is interesting to compare the resummed HT cross sections with the ones obtained in the framework of the frozen coupling approximation. In *Fig.2*, the ratio  $r_M = (\Sigma_M^{HT})^{res}/(\Sigma_M^{HT})^o$  for negatively charged particles ( $\pi^-$ ,  $K^-$ ) is shown. In the computing of  $(\Sigma_M^{HT})^o$  we have neglected the meson's w.f. dependence on the scale  $\hat{Q}^2$ . Let us emphasize that for the kaon we have used the frozen coupling version of our expression (9), but not the Bagger-Gunion formula from [6], which is incorrect in that case.

As is seen from *Fig.2(a)*,  $r_{\pi^-} \simeq 1$  almost for all  $p_T$ , whereas  $r_{K^-}$  falls from  $r_{K^-} \simeq 2.75$  at  $p_T = 2 \text{ GeV}/c$ ,  $y = 0$  until  $r_{K^-} \simeq 2.13$  at  $p_T = 11 \text{ GeV}/c$ ,  $y = 0$  and from  $r_{K^-} \simeq 2.71$  at  $p_T = 2 \text{ GeV}/c$ ,  $y = 0.5$  till  $r_{K^-} \simeq 1.5$  at  $p_T = 11 \text{ GeV}/c$ ,  $y = 0.5$ . For  $K^-$  this ratio demonstrates also a sharp dependence on  $y$  at fixed  $\sqrt{s}$ ,  $p_T$  (*Fig.2(b)*).

In all of the following figures we have used the resummed expression for the HT cross section. In *Fig.3* the ratio  $R_M = |\Delta_M^{HT}/\Delta_M^{LT}|$  is depicted. For all particles the LT cross section difference is positive  $\Delta_M^{LT} > 0$ , since  $\Sigma_{M^+}^{LT} \sim u_p(x, -\hat{t})e_u^2$ , while  $\Sigma_{M^-}^{LT} \sim d_p(x, -\hat{t})e_d^2$ . The smaller quark charge  $e_d$  and the smaller distribution function  $d_p$  both suppress  $\Sigma_{M^-}^{LT}$  [6]. The HT cross section difference may change sign at small  $p_T$  and become negative  $\Delta_M^{HT} < 0$ . For example,  $\Delta_{\pi^-}^{HT} < 0$  at  $2 \text{ GeV}/c \leq p_T \leq 11 \text{ GeV}/c$  for  $\sqrt{s} = 25 \text{ GeV}$ ,  $y = 0$  and at  $2 \text{ GeV}/c \leq p_T \leq 9 \text{ GeV}/c$  for  $\sqrt{s} = 25 \text{ GeV}$ ,  $y = 0.5$ . Only at the phase-space boundary  $p_T > 11 \text{ GeV}/c$  in the first case or at  $p_T > 9 \text{ GeV}/c$  in the second one  $\Sigma_{\pi^+}^{HT} > \Sigma_{\pi^-}^{HT}$ . Therefore, we plot the absolute value of  $R_M$ . The similar picture has been also found for other mesons.

As is seen from *Figs.3(a), (b)* for pion and kaon the HT contribution is comparable with the LT one only at  $p_T \leq 3 \text{ GeV}/c$ . We do not find a considerable and stable growth of HT contributions at large values of  $p_T$  for all the cross section differences  $\Delta_M^{HT}$  ( $M = \pi, K$ ), as well as, for all  $\Sigma_M^{HT}$ . Thus,  $\Sigma_{K^-}^{HT}/\Sigma_{K^-}^{LT}$  is small at

high  $p_T$  for different  $\sqrt{s}$  (*Fig.4(a)*). At the same time  $\Sigma_{K^+}^{HT}/\Sigma_{K^+}^{LT}$  is a rising function of  $p_T$  for  $p_T > 4 \text{ GeV}/c$  ( $\sqrt{s} = 14.1 \text{ GeV}$ ) and  $p_T > 7 \text{ GeV}/c$  ( $\sqrt{s} = 25 \text{ GeV}$ ).

The cross section differences  $\Delta_M^{LT}$  and  $\Delta_M^{tot} = \Delta_M^{LT} + \Delta_M^{HT}$  as functions of  $p_T$  are shown in *Fig.5*. For the pion the total cross section difference  $\Delta_\pi^{tot}$  in the region of small  $p_T$  is smaller than  $\Delta_\pi^{LT}$  due to  $\Delta_\pi^{HT} < 0$  in this region (*Fig.5(a)*). But for kaon  $\Delta_K^{tot} > \Delta_K^{LT}$  in the same kinematic domain. For both mesons the difference between  $\Delta_M^{tot}$  and  $\Delta_M^{LT}$  cross sections is small.

The rapidity dependence of  $R_M$  at  $\sqrt{s} = 25 \text{ GeV}$ ,  $p_T = 3 \text{ GeV}/c$  plotted in *Fig.3(c)* illustrates not only the tendency of the HT contributions to be enhanced in the region of negative rapidity, but also reveals an interesting feature of the HT terms; as is seen from *Fig.3(c)* the ratio  $R_M$  is an oscillating function of the rapidity. This property of the HT terms may have important phenomenological consequences. In fact, in *Fig.6* we have depicted  $\Delta_M^{tot}$  and  $\Delta_M^{LT}$  versus rapidity. In both cases, owing to observed property of  $\Delta_M^{HT}(y)$ , in certain domains of the rapidity interval  $-2 \leq y \leq 2.105$  the total cross section difference is more than  $\Delta_M^{LT}$  and in some ones less than  $\Delta_M^{LT}$ . In the case of the kaon photoproduction

$$\begin{aligned} \Delta_K^{tot} > \Delta_K^{LT}, \quad \text{for } -2 \leq y \leq 0.3 \quad \text{and} \quad 1.8 \leq y \leq 2.105, \\ \Delta_K^{tot} < \Delta_K^{LT}, \quad \text{for } 0.3 \leq y \leq 1.8. \end{aligned}$$

The properties of the HT terms found in the pion and kaon photoproduction processes persist also in the  $\rho$ -meson photoproduction. But now the HT contributions change the whole picture of the process arising from the ordinary LT calculations. Thus, as in the case of the pion photoproduction, the HT terms are enhanced relative to the leading ones and  $\Delta_\rho^{HT} < 0$  almost for all  $p_T$ . But now  $|\Delta_\rho^{HT}|$  takes such large values that it even changes the sign of the total cross section difference. That is, if in accordance with the LT estimations  $\Sigma_{\rho^+}^{tot} > \Sigma_{\rho^-}^{tot}$  must be valid for all  $p_T$ , for  $p_T < p_T^c$  we find  $\Sigma_{\rho^+}^{tot} < \Sigma_{\rho^-}^{tot}$ . The value of  $p_T^c$  depends on the process parameters, as well as on the  $\rho$ -meson w.f. used in calculations. At  $p_t \approx p_T^c$  we have  $\Sigma_{\rho^+}^{tot} \approx \Sigma_{\rho^-}^{tot}$ .

Our results are shown in *Fig.7*. For the parameters indicated in the figure a critical value of  $p_T$  is:  $p_{T1}^c \simeq 5.05 \text{ GeV}/c$  for CZ w.f., and  $p_{T2}^c \simeq 6.25 \text{ GeV}/c$  for BB w.f. In all kinematic domains the HT contributions found using BB w.f. exceed the ones obtained by applying CZ w.f., that is,  $|\Delta_\rho^{HT}(BB)| > |\Delta_\rho^{HT}(CZ)|$ . For example, the ratio  $|\Delta_\rho^{HT}(BB)/\Delta_\rho^{HT}(CZ)|$  equals to 2.39 at  $\sqrt{s} = 25 \text{ GeV}$ ,  $p_T = 5 \text{ GeV}/c$ ,  $y = 0$ , or to 2.63 at  $\sqrt{s} = 25 \text{ GeV}$ ,  $p_T = 3 \text{ GeV}/c$ ,  $y = -1$ . Our results confirm the conclusion made by the authors in [13] concerning a possibility of increasing the rate of the production of transversely polarized  $\rho$ -meson. Similar pictures persist in *Fig.8*, where  $\Delta_\rho^{LT}$  and  $\Delta_\rho^{tot}$  are depicted as functions of the rapidity  $y$ . In *Fig.8(a)*, for the process parameters  $\sqrt{s} = 25 \text{ GeV}$ ,  $p_T = 3 \text{ GeV}/c$  we have: in domain  $I'$  ( $-1.74 \leq y \leq 1.3$ ) the total cross section difference for CZ w.f. is negative, in  $I$  ( $-1.5 \leq y \leq 1.5$ ) -  $\Delta_\rho^{tot}(BB) < 0$ . In *Fig.8(b)* the same is shown for  $\sqrt{s} = 25 \text{ GeV}$ ,  $p_T = 5 \text{ GeV}/c$ . In two other regions lying outside of

$I(I')$  the  $\Sigma_{\rho^+}^{tot}$  exceeds  $\Sigma_{\rho^-}^{tot}$  (for  $-2 \leq y \leq -1.5$ ,  $\Sigma_{\rho}^{tot}(BB)$  and for  $-2 \leq y \leq -1.74$ ,  $\Sigma_{\rho}^{tot}(CZ)$  are negligible and are not shown).

It is worth noticing that in [6] the authors considered the  $\rho$ -meson photoproduction at the same process's parameters and predicted  $\Sigma_{\rho}^{tot} < 0$  at  $p_T \leq 3 \text{ GeV}/c$ , but could not find similar effects for  $\Sigma_{\rho}^{tot}$  in dependence on the rapidity. Our investigations prove that  $\Sigma_{\rho}^{tot} < 0$  at  $p_T < p_T^c$  and  $p_T^c$  well into deep perturbative domain. We have also demonstrated that the same phenomenon exists for  $y_1^c \leq y \leq y_2^c$ .

## 6 CONCLUDING REMARKS

In this work we have calculated the single meson inclusive photoproduction via higher twist mechanism and obtained the expressions for the subprocess  $\gamma q \rightarrow Mq$  cross section for mesons with both symmetric and non-symmetric wave functions. For the calculation of the cross section we have applied the running coupling constant method and revealed IR renormalon poles in the cross section expression. IR renormalon induced divergences have been regularized by means of the principal value prescription and the resummed expression (the Borel sum) for the higher twist cross section has been found. Phenomenological effects of the obtained results have been discussed.

Summing up we can state that:

- i) for mesons with non-symmetric w.f. in the framework of the frozen coupling approximation the higher twist subprocess cross section cannot be normalized in terms of a meson electromagnetic form factor;
- ii) in the context of the running coupling constant method the HT subprocess cross section cannot be normalized in terms of meson's elm form factor neither for mesons with symmetric w.f. nor for non-symmetric ones;
- iii) the resummed HT cross section differs from that found using the frozen coupling approximation, in some cases, considerably;
- iv) HT contributions to the single meson photoproduction cross section have important phenomenological consequences, specially in the case of  $\rho$ -meson photoproduction. In this process the HT contributions wash the LT results off, changing the LT predictions.

## ACKNOWLEDGMENTS

The author would like to thank the International Centre for Theoretical Physics, Trieste, for hospitality and Prof. S. Randjbar-Daemi for his interest in this work.

## REFERENCES

1. S.J.Brodsky, R.Blankenbecler and J.F.Gunion: Phys.Rev.D6, 2651 (1972);  
S.J.Brodsky and G.R.Farrar: Phys.Rev.Lett.31, 1153 (1973).
2. G.P.Lepage and S.J.Brodsky: Phys.Rev.D22, 2157 (1980).
3. V.L.Chernyak and A.R.Zhitnitsky: Phys.Rep.112, 173 (1980).
4. S.S.Agaev: Phys.Lett. B283, 125(1992); Z.Phys.C-Particles and Fields57, 403 (1993);  
E.L.Berger and S.J.Brodsky: Phys.Rev.Lett. 42, 940 (1979);  
E.L.Berger: Z.Phys.C-Particles and Fields 4, 289 (1980).
5. V.N.Baier and A.G.Grozin: Phys.Lett.B96, 181 (1980);  
S.Gupta: Phys.Rev.D24, 1169 (1981).
6. J.A.Bagger and J.F.Gunion: Phys.Rev.D25, 2287 (1982).
7. J.A.Hassan and J.K.Storrow: Z.Phys.C-Particles and Fields14, 65 (1982).
8. S.J.Brodsky, G.P.Lepage and P.B.Mackenzie: Phys.Rev.D28, 228 (1983).
9. R.D.Field, R.Gupta, S.Otto and L.Chang: Nucl.Phys.B186, 429 (1981).
- 10.S.S.Agaev: Phys.Lett.B360, 117 (1995); E. Phys.Lett.B369, 379 (1996);  
S.S.Agaev: Mod.Phys.Lett.A10, 2009 (1995).
- 11.S.S.Agaev: Mod.Phys.Lett.A11, 957 (1996); ICTP preprint IC/95/291, September 1995, hep-ph/9611215.
- 12.A.H.Mueller: Nucl.Phys.B250, 327 (1985);  
H.Contopanagos and G.Sterman: Nucl.Phys. B419, 77 (1994).
- 13.P.Ball and V.M.Braun: Phys.Rev.D54, 2182 (1996).
- 14.S.S.Agaev: Int.J.Mod.Phys.A8, 2605 (1993); Int.J.Mod.Phys.A9, 5077 (1994).
- 15.G.'t Hooft: In: The Whys of Subnuclear Physics, Proc.Int.School, Erice, 1977, ed. A.Zichichi, Plenum, New York, 1978;  
V.I.Zakharov: Nucl.Phys.B385, 452 (1982).
- 16.A.Erdelyi: Higher transcendental functions, v.2, McGraw-Hill Book Company, New York, 1953.
- 17.M.Neubert: Phys.Rev.D51, 5924 (1995);  
P.Ball, M.Beneke and V.M.Braun: Nucl.Phys.B452, 563 (1995);  
P.Ball, M.Beneke and V.M.Braun: Phys.Rev.D52, 3929 (1995);  
M.Beneke and V.M.Braun: Phys.Lett.B348, 513 (1995);  
C.N.Lovett-Turner and C.J.Maxwell: Nucl.Phys.B452, 188 (1995).

**18.**P.Aurenche, R.Baier, A.Douiri, M.Fontannaz and D.Schiff: Nucl.Phys.B286, 553 (1987).

**19.**J.F.Owens: Phys.Lett.B266, 126(1991).

**20.**J.F.Owens: Phys.Rev.D19, 3279 (1979);

J.F.Owens, E.Reya and M.Glück: Phys.Rev.D18, 1501 (1978).

**21.**J.Binnewies, G.Kramer and B.A.Kniehl: DESY preprint DESY-95-048, March 1995.

## FIGURE CAPTIONS

**Fig.1** Feynman diagrams contributing to the higher twist subprocess  $\gamma q \rightarrow Mq$ . Here  $\mathbf{p}$  and  $\mathbf{P}$  are the hadron  $h$  and meson  $M$  four momenta, respectively.

**Fig.2** Ratio  $r_M = (\Sigma_M^{HT})^{res}/(\Sigma_M^{HT})^o$ , where  $(\Sigma_M^{HT})^{res}$  and  $(\Sigma_M^{HT})^o$  are HT contributions to the photoproduction cross section calculated using the running and frozen coupling approximations, respectively. The ratio is depicted as a function of  $p_T$  a), and of the rapidity b).

**Fig.3** Ratio  $R_M = |\Delta_M^{HT}/\Delta_M^{LT}|$  for the pion a), and for the kaon b) at fixed rapidity  $y=0$ . In c)  $R_M$  is plotted as a function of  $y$  for the pion (dashed curve) and for the kaon (solid curve).

**Fig.4** The dependence of the ratio  $\Sigma_K^{HT}/\Sigma_K^{LT}$  for  $K^+$  and  $K^-$  on  $p_T$  a) and on  $y$  b).

**Fig.5** The cross section difference  $\Delta_M$  is shown at fixed rapidity for pions a), and for kaons b). For the curves **1** the process c.m. energy is  $\sqrt{s} = 14.1 \text{ GeV}$ , for the curves **2** -  $\sqrt{s} = 25 \text{ GeV}$ .

**Fig.6** The cross section difference  $\Delta_M$  as a function of the rapidity for pions a); for kaons b).

**Fig.7**  $\Delta_\rho$  for  $\rho$ -meson. The solid curve describes  $\Delta_\rho^{LT}$ , whereas the dashed curves correspond to  $\Delta_\rho^{tot}$ . The long-dashed curve has been obtained using the CZ w.f., the short-dashed one- BB w.f. In the domains  $I(BB \text{ w.f.})$  and  $I'(CZ \text{ w.f.})$  the absolute value of  $|\Sigma_\rho^{tot}|$  or  $\Sigma_\rho^{tot} - \Sigma_\rho^{tot}$  is plotted.

**Fig.8**  $\Delta_\rho$  dependence on the rapidity at  $\sqrt{s} = 25 \text{ GeV}, p_T = 3 \text{ GeV}/c$  for a); at  $\sqrt{s} = 25 \text{ GeV}, p_T = 5 \text{ GeV}/c$  for b). The solid curve corresponds to  $\Delta_\rho^{LT}$ , the long-dashed and short-dashed curves describe  $\Delta_\rho^{tot}$  obtained using CZ and BB w.f., respectively. In regions  $I(BB \text{ w.f.})$  and  $I'(CZ \text{ w.f.})$  the cross section difference  $\Sigma_\rho^{tot} - \Sigma_\rho^{tot}$  is shown.

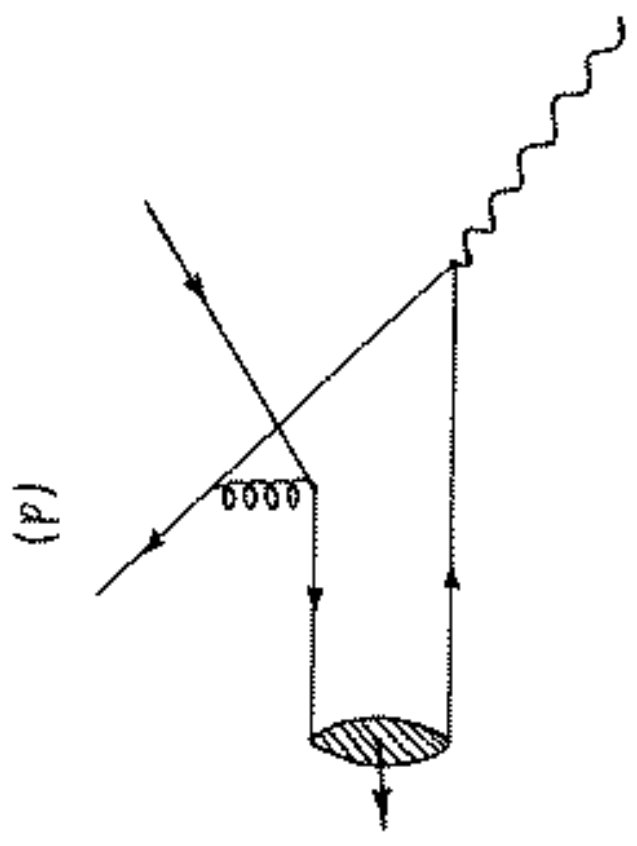
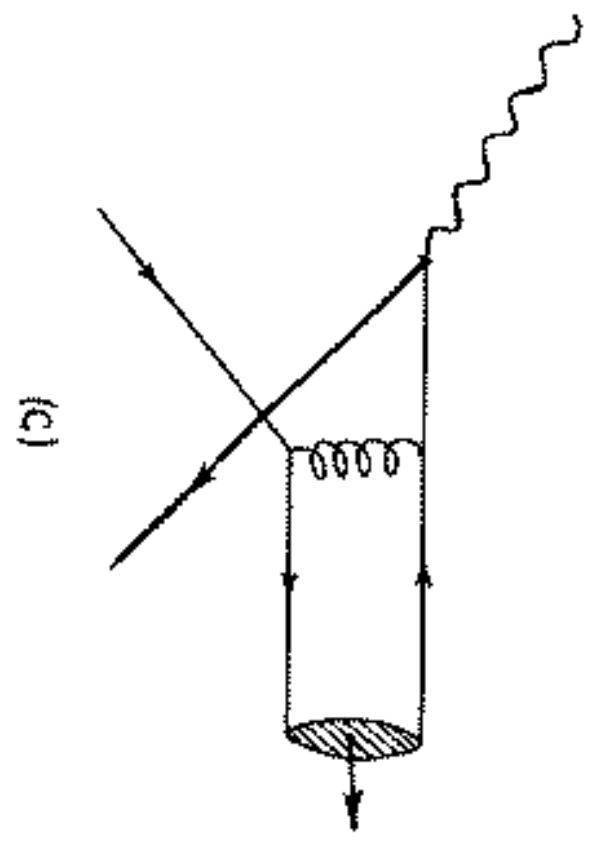
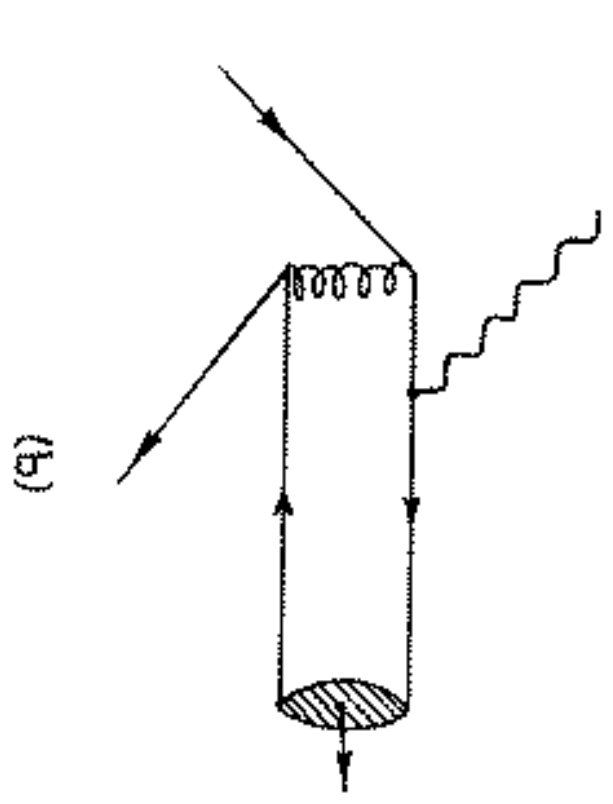
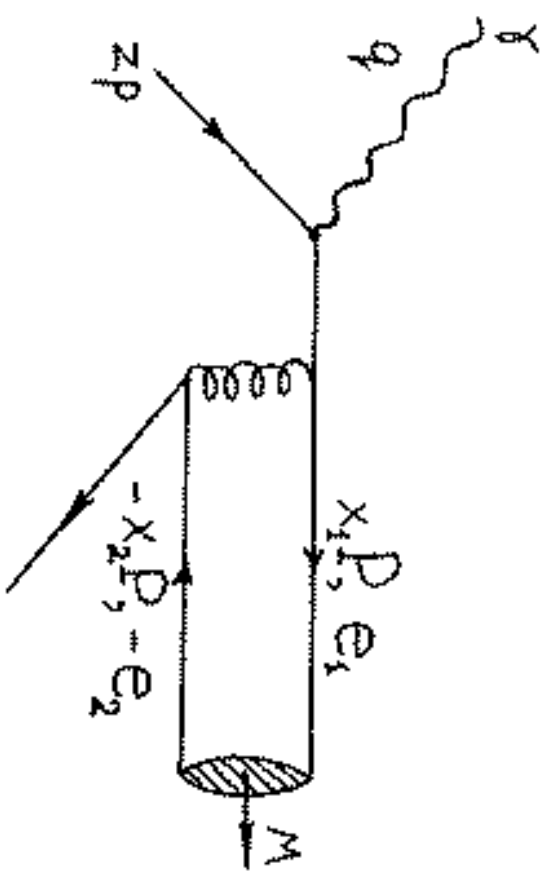


Fig. 1

Fig.2

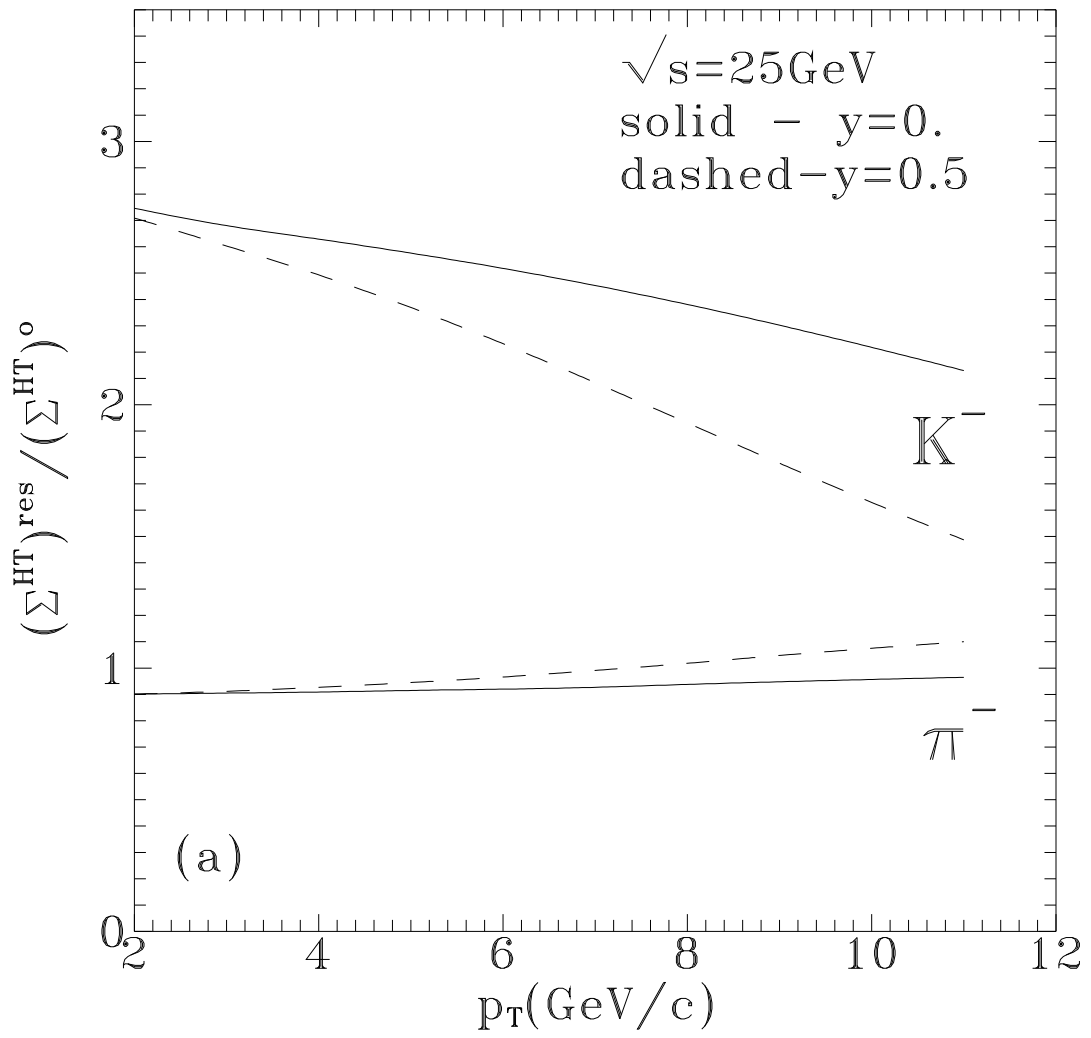


Fig.2

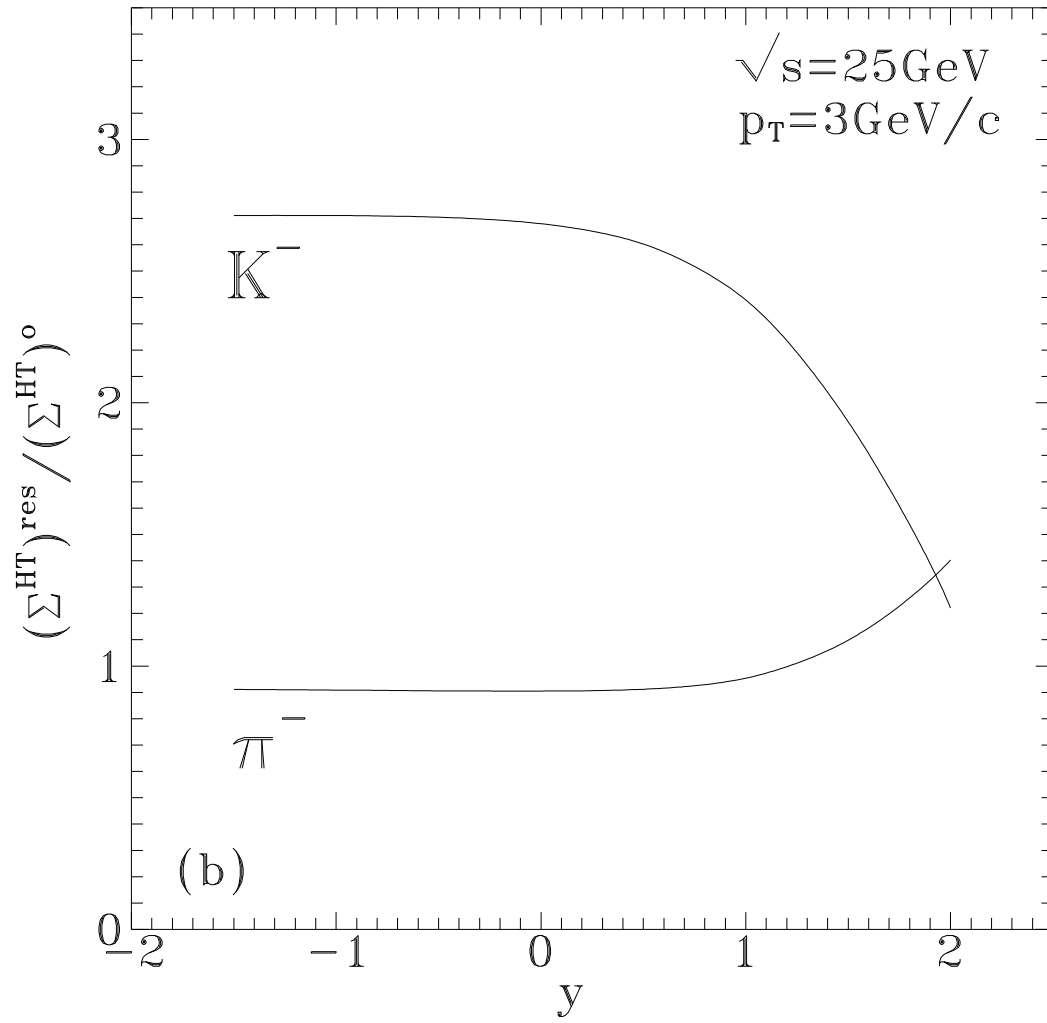


Fig.3

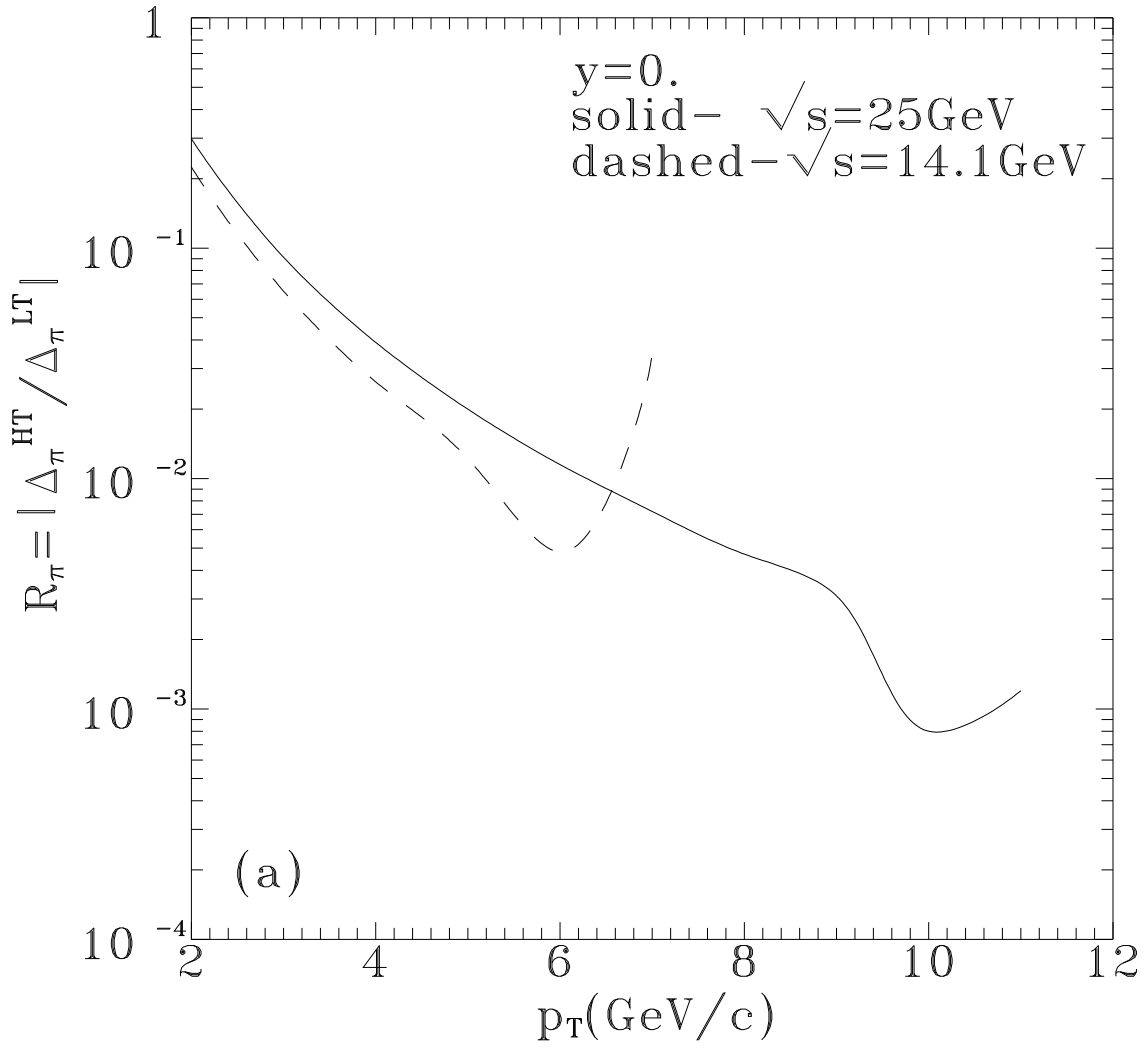


Fig.3

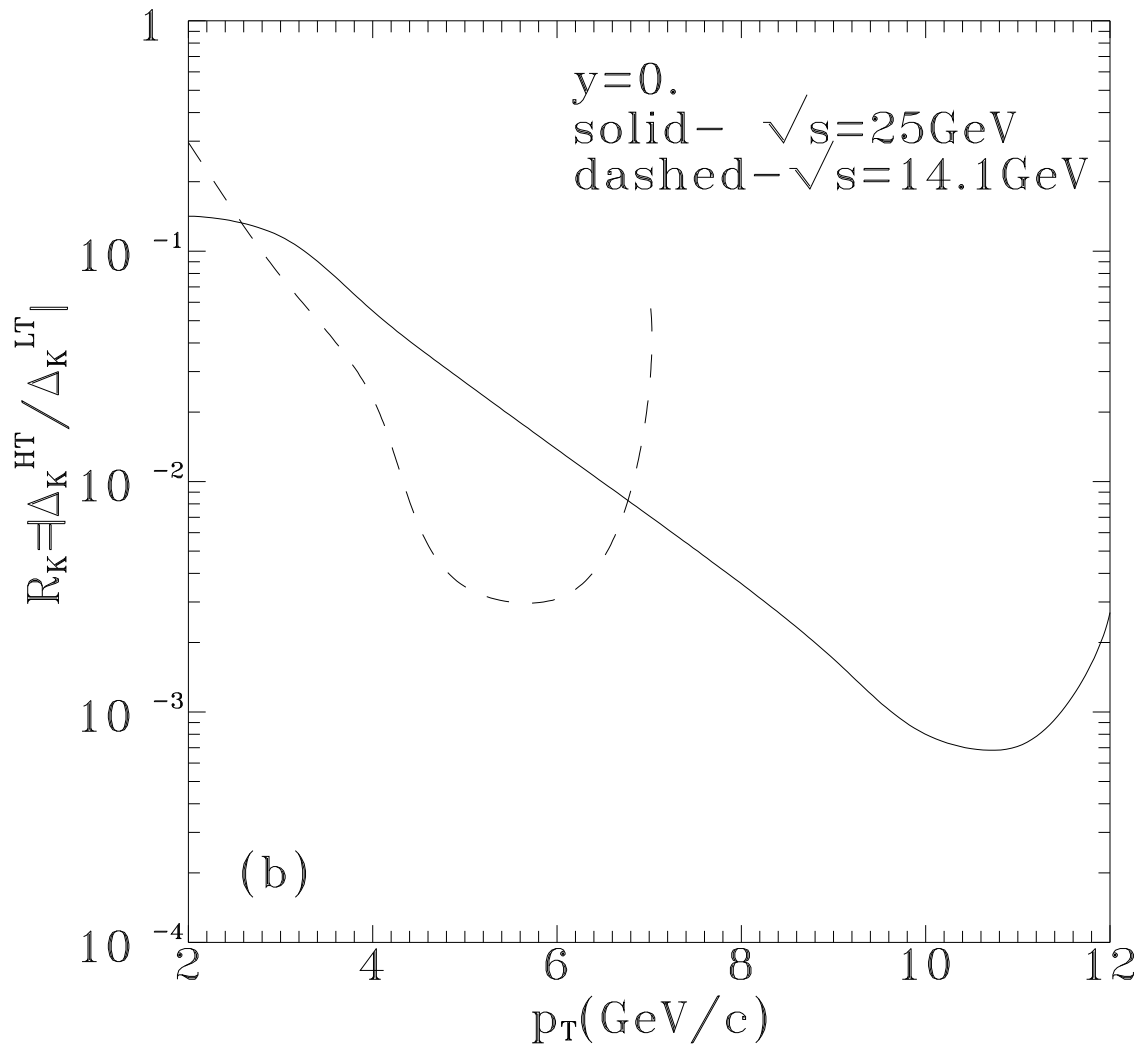


Fig.3

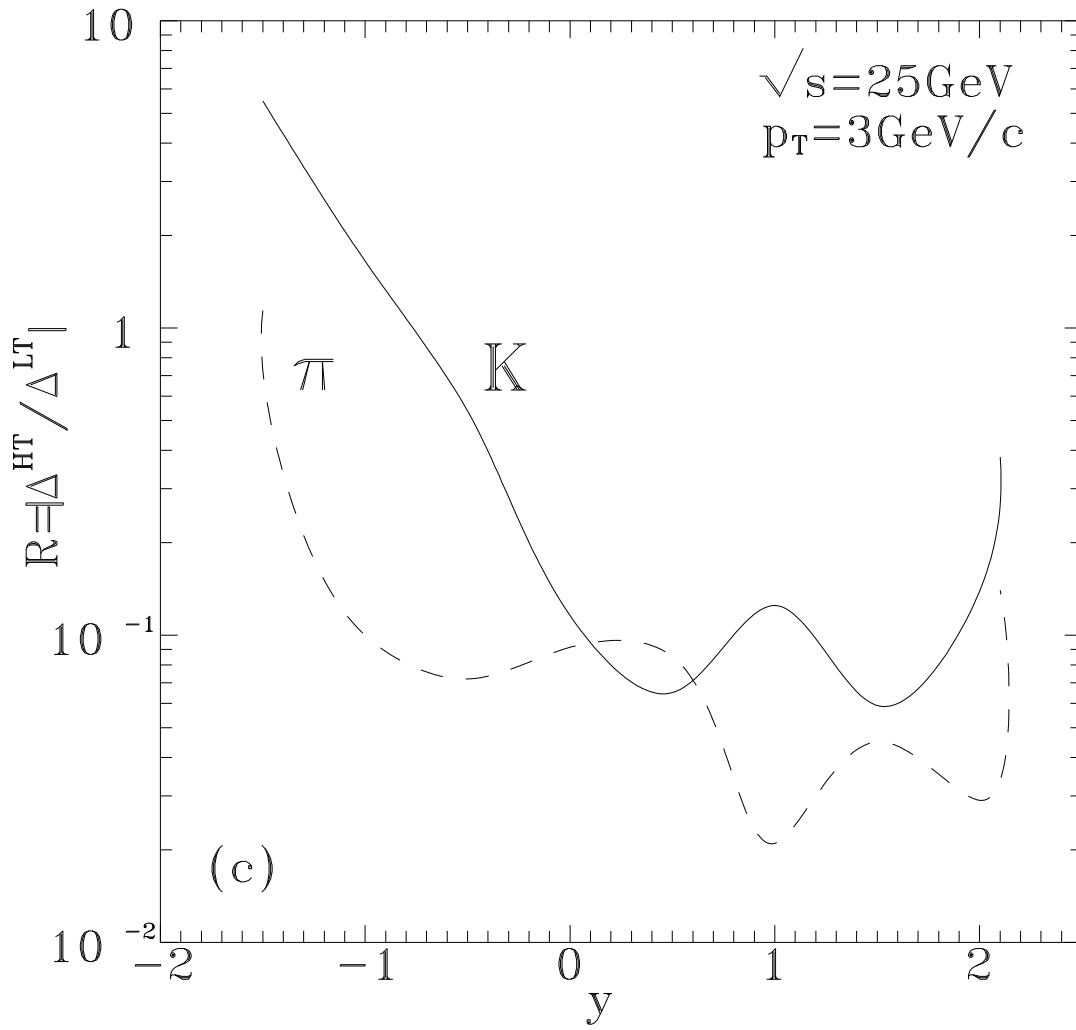


Fig.4

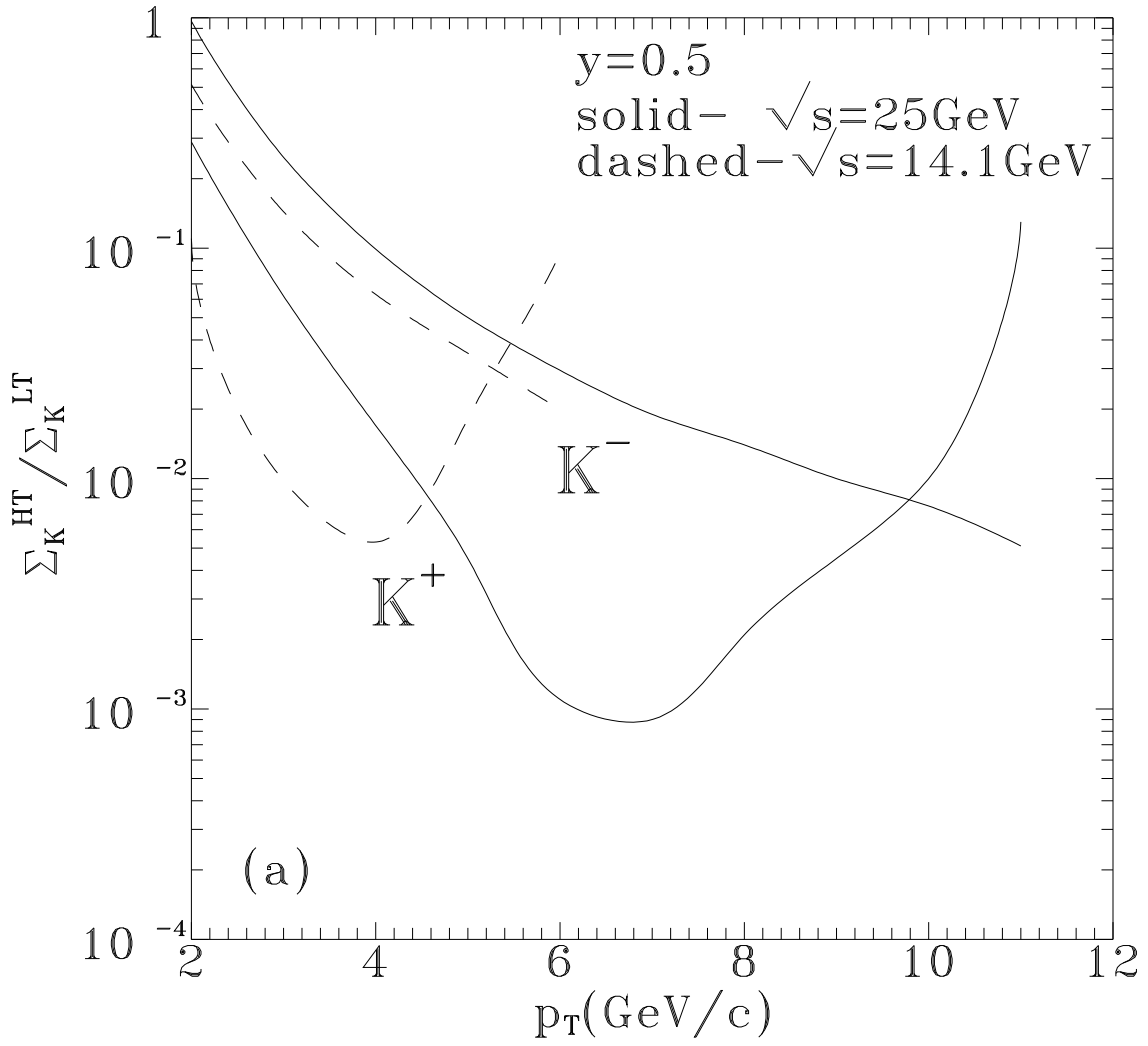
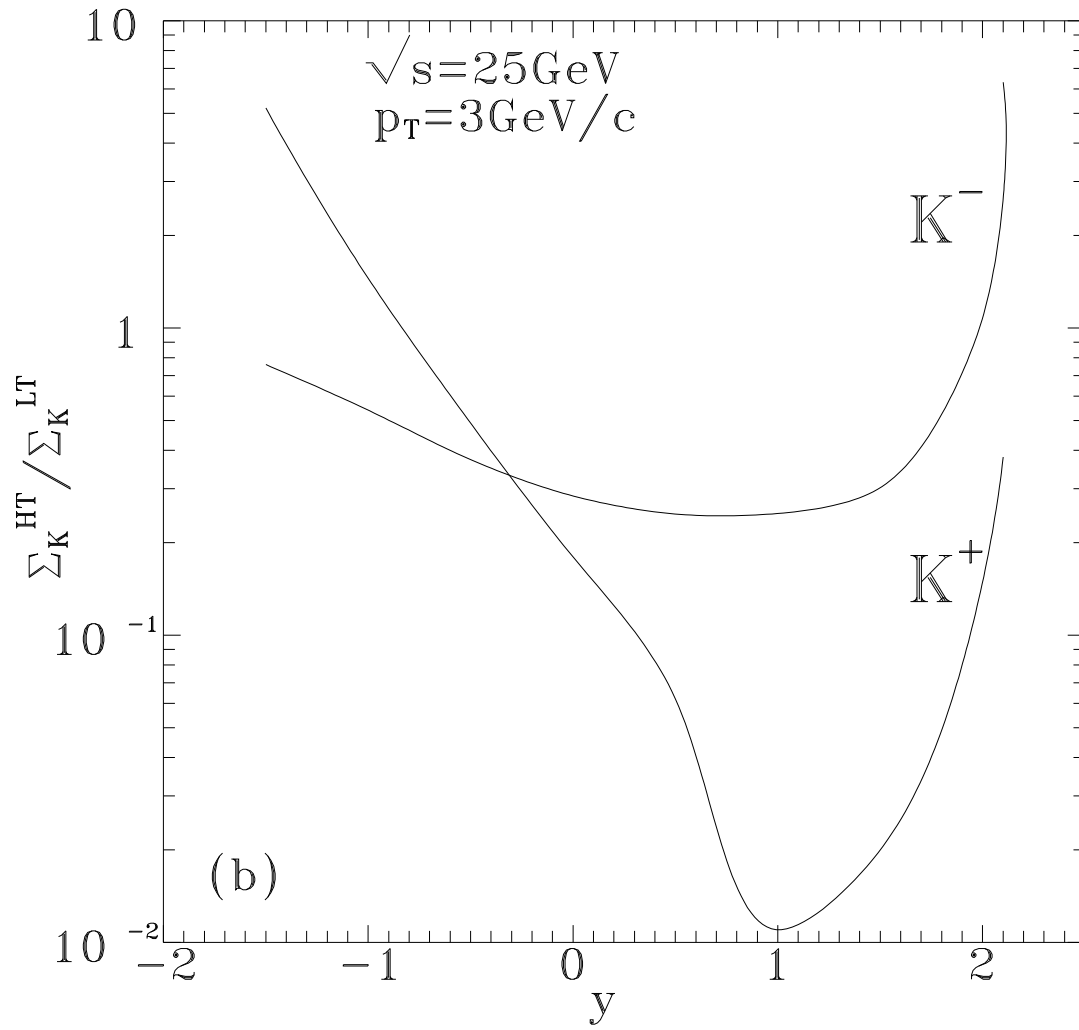


Fig.4



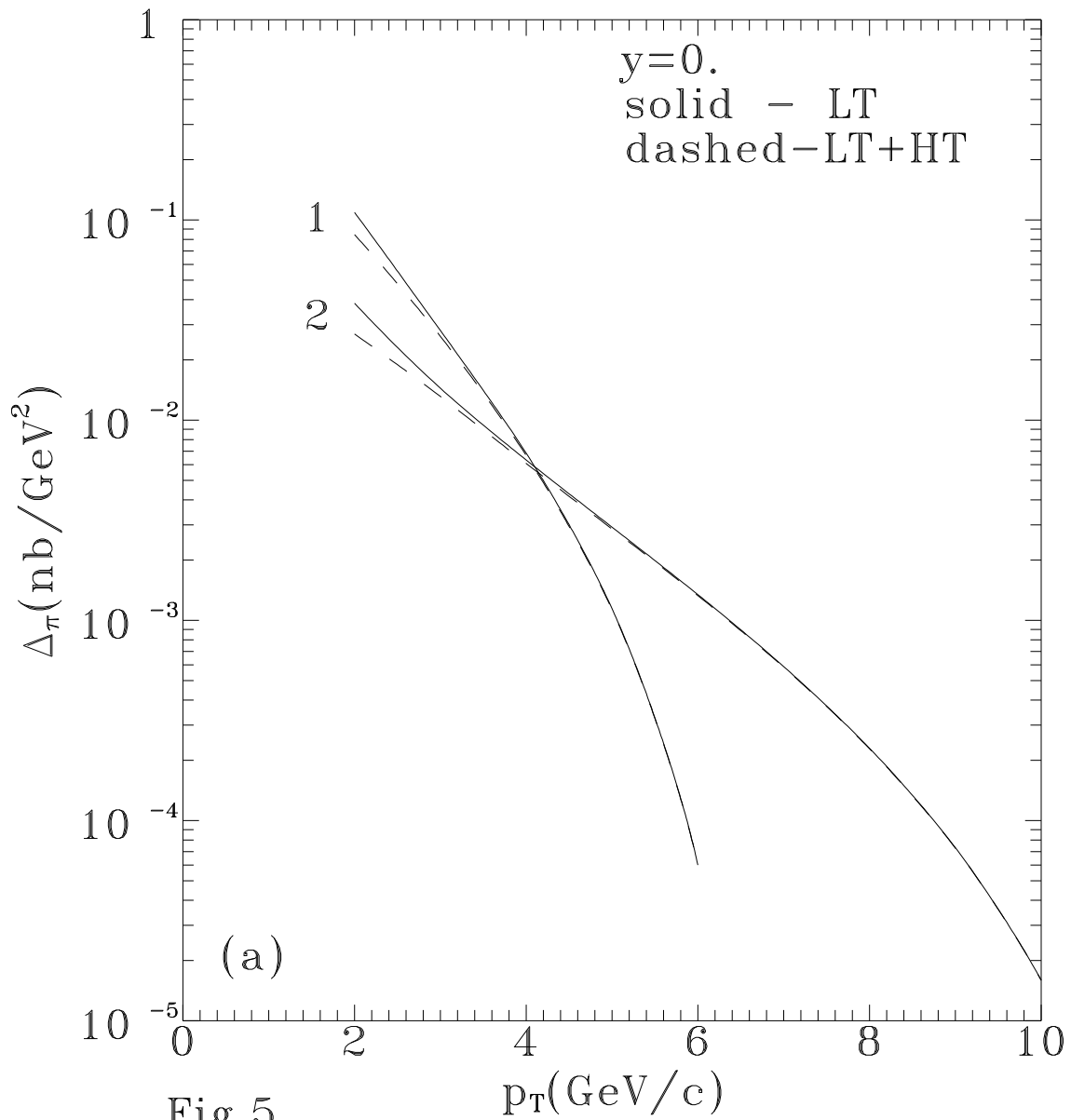


Fig.5

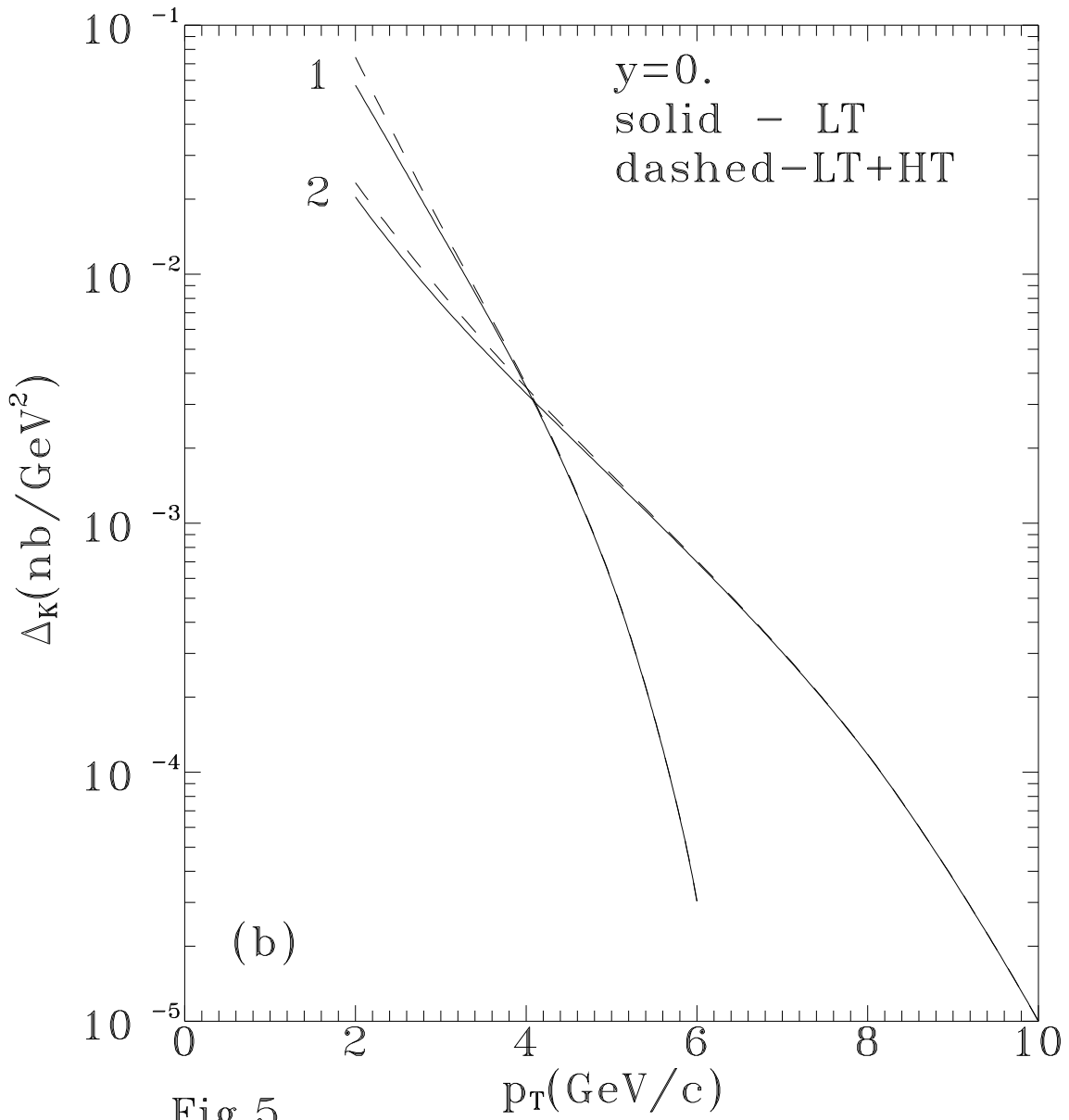


Fig.5

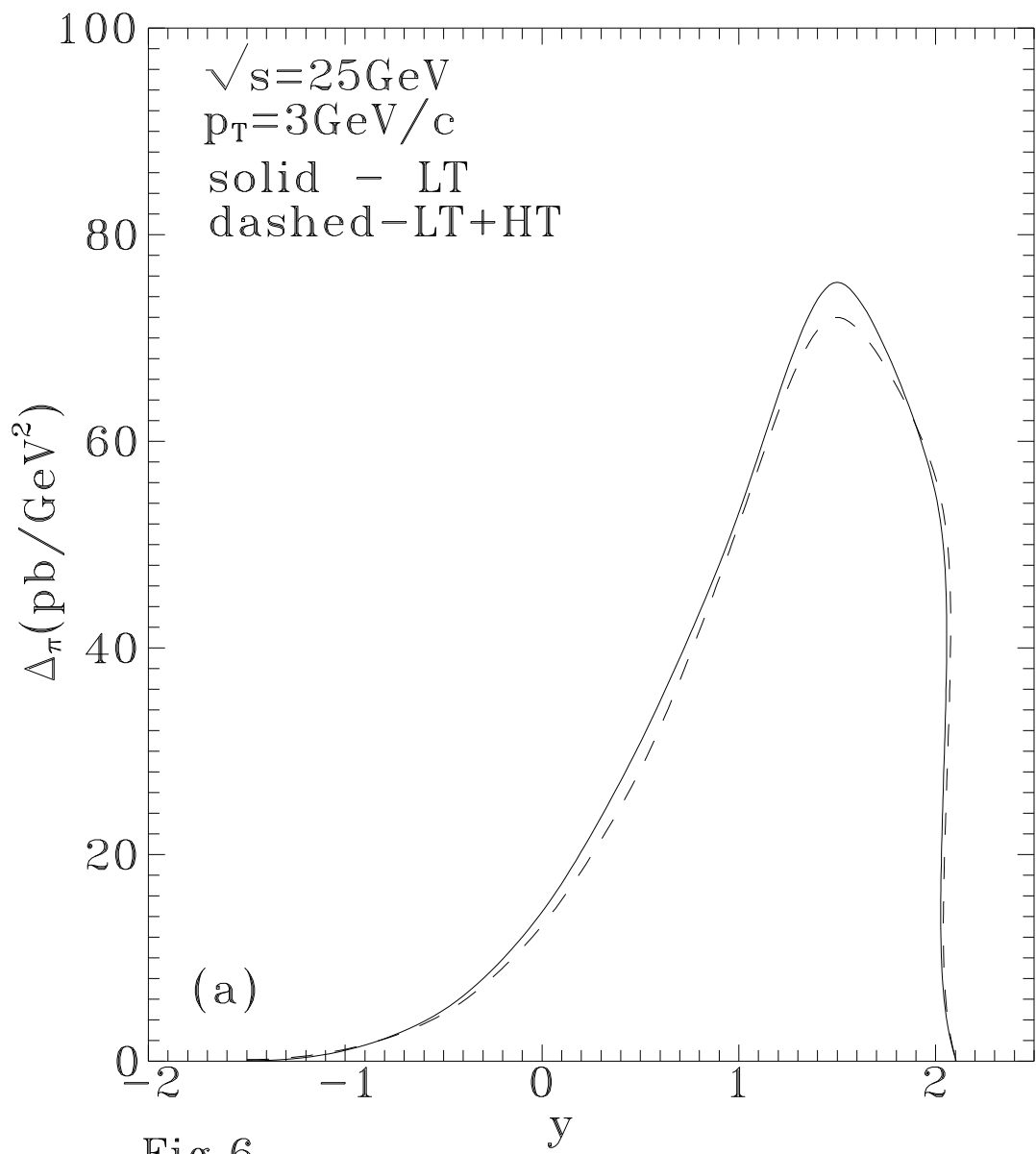


Fig.6

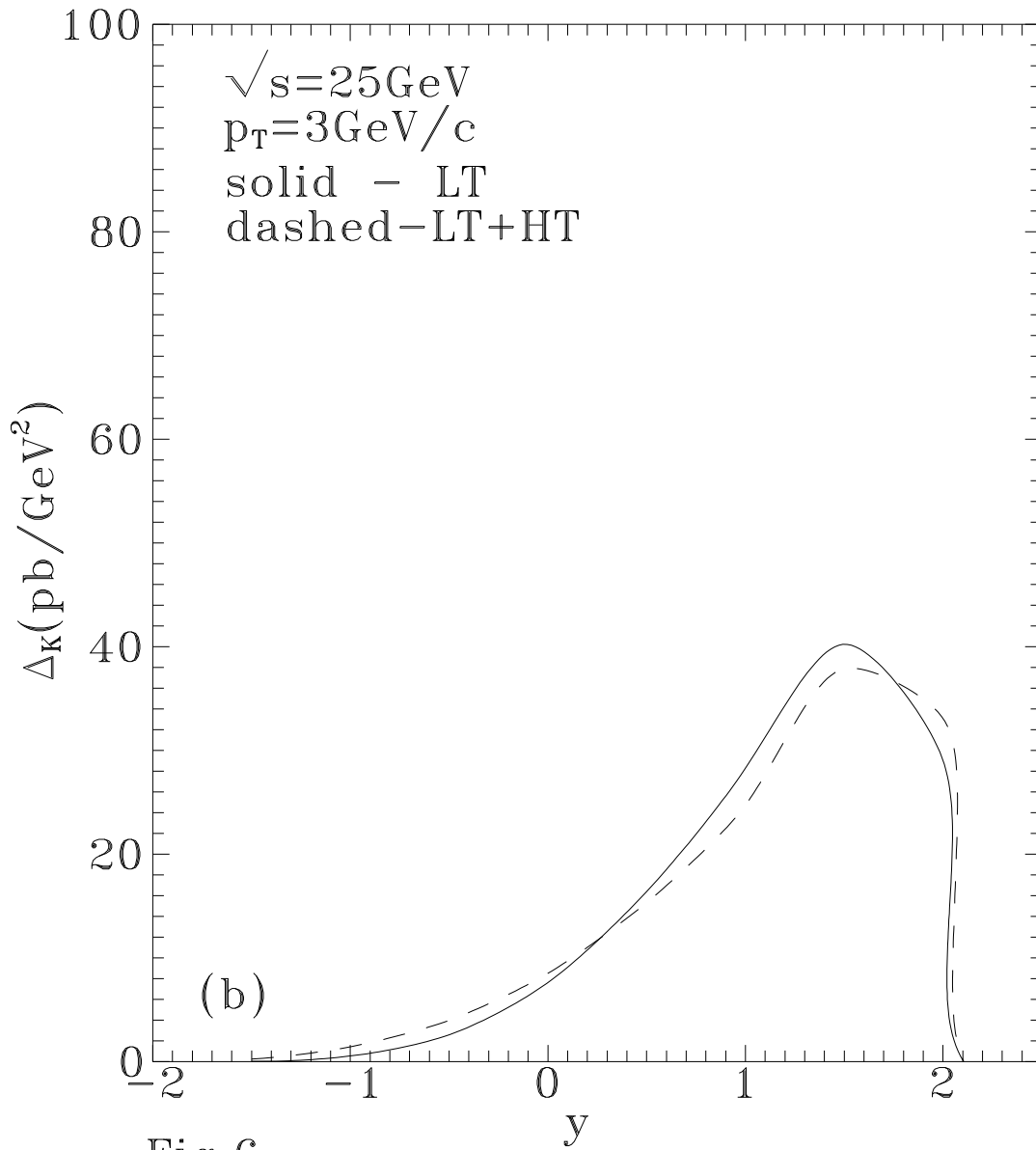
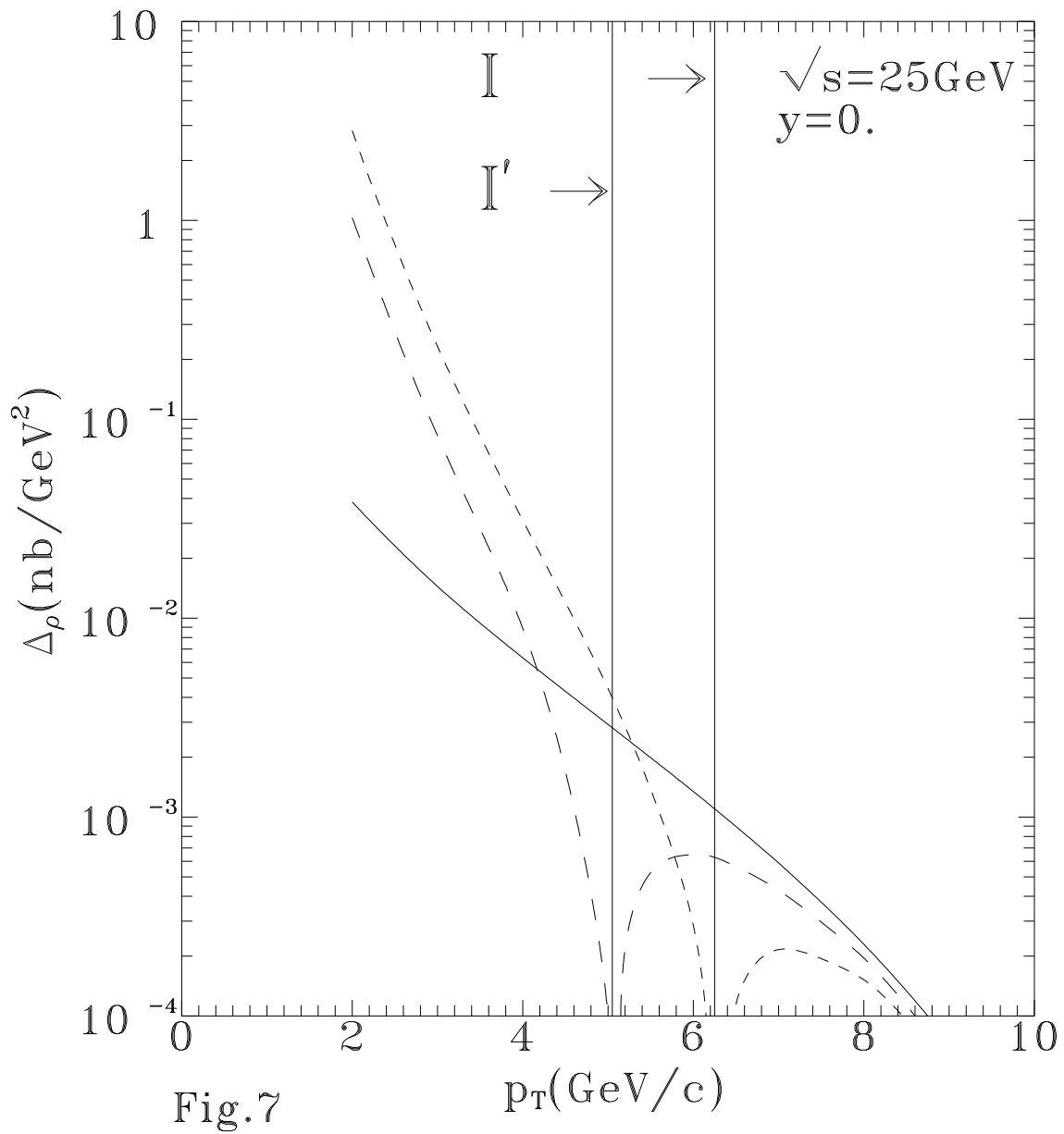


Fig.6



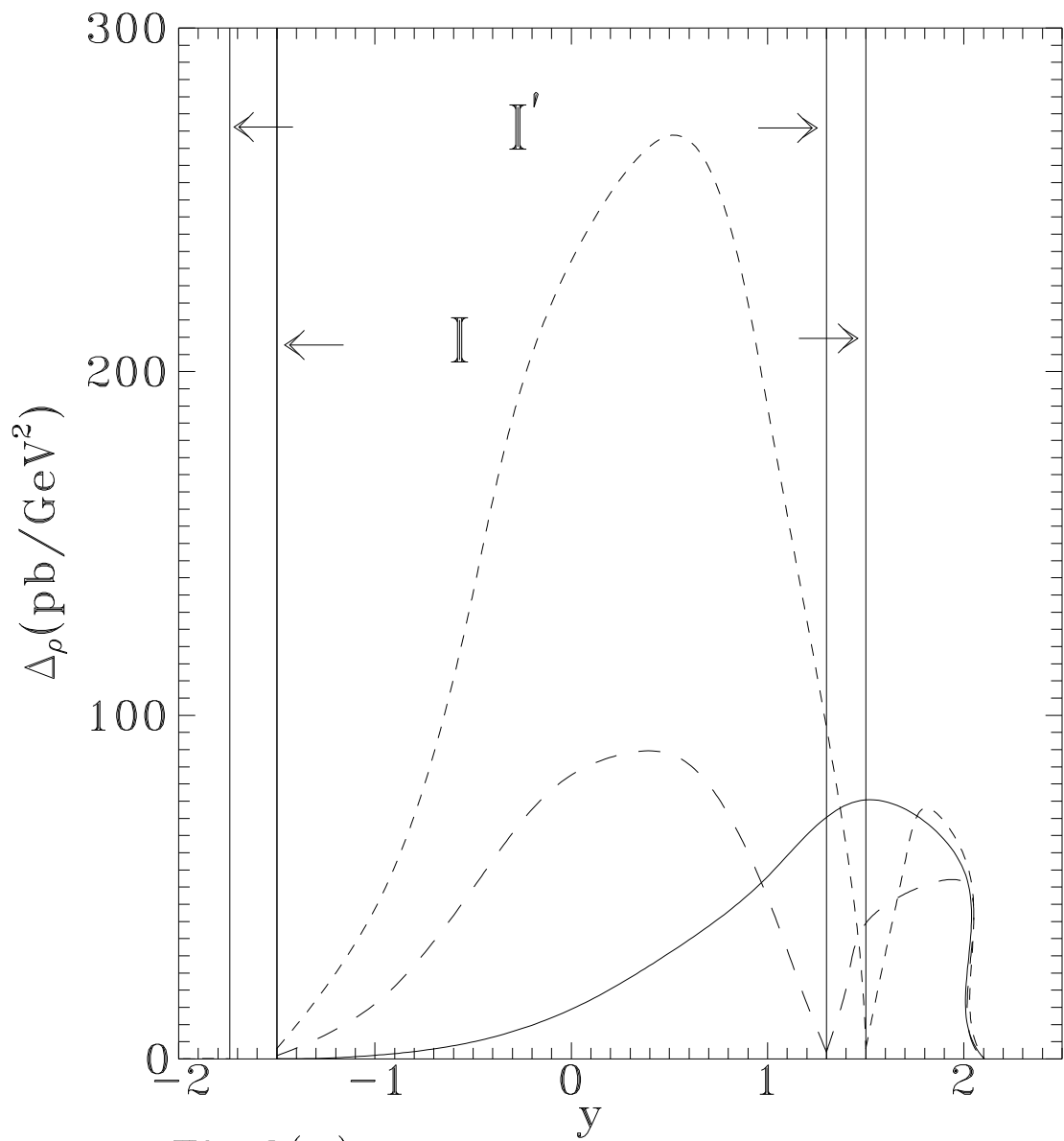


Fig.8(a)

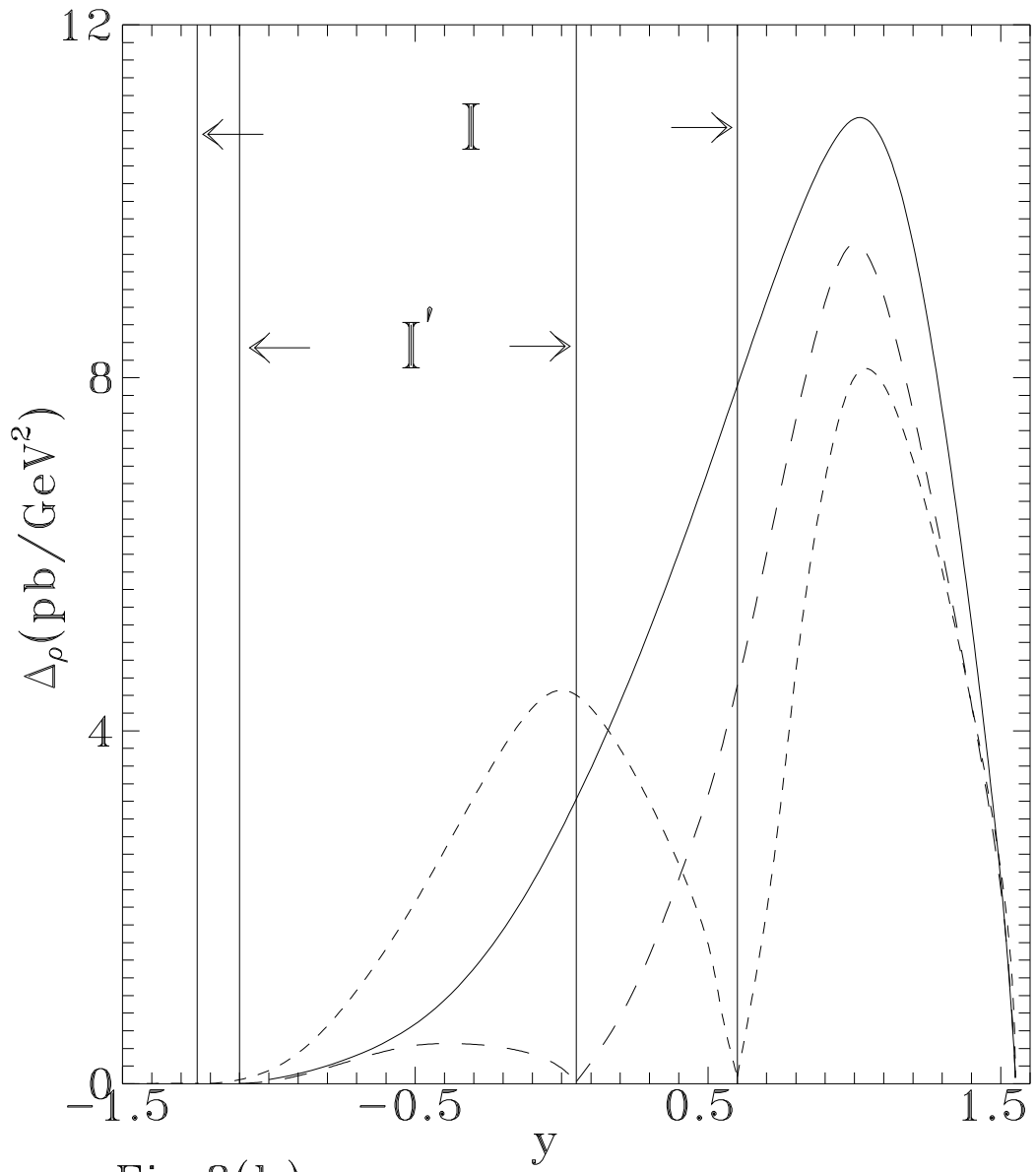


Fig.8(b)